Electronic Supplementary Material (ESI) for New Journal of Chemistry.

Deciphering the positional impact of chlorine in new series of berberine analogues towards superb-selective "turn-on" hydrophobic signaling of bovine serum albumin at physiological pH

Gopal Chandra Jana[a], Sk. Nayim[a], Nandan Kumar Sahoo[a], Somnath Das[a], Mt. Nasima Aktara[a], Anirudha Patra [a], Md. Maidul Islam[b], and Maidul Hossain*[a]

[a] Department of Chemistry and Chemical Technology, Vidyasagar University, Midnapore, 721102, West Bengal, India.

[b] Department of Chemistry, Aliah University, Kolkata, West Bengal, India.

Corresponding author: Dr. Maidul Hossain[a], Assistant Professor, Department of Chemistry and Chemical Technology, Vidyasagar University, Midnapore, 721102, West Bengal, India. Mobile no: 9432976277. Email address: hossainm@mail.vidyasagar.ac.in

Anisotropy (r) calculation:

The steady state anisotropy (r) of various synthesized analogue were calculated in absence and in presence of BSA by the equation given below [45]

$$r = \frac{I_{VV} - GI_{VH}}{I_{VV} + 2GI_{VH}} \quad (1)$$

where, I_{VV} is the emission intensity when excitation and emission polariser are vertically oriented, I_{VH} is the emission intensity when excitation and emission polariser are horizontally oriented and G, the instrumental grating factor is described as [45]

$$G = \frac{I_{HV}}{I_{HH}} \quad (2)$$

Calculation of non-radiative decay rate constant (k_{nr}): The non-radiative rate constant of berberine analogue in absence and in presence of BSA was calculated by subsequent equation[3]

$$k_{nr} = k_r\left[\frac{1}{\Phi} - 1\right] \quad (3)$$

Where k_r is the radiative rate constant and is the quantum yield of the synthesized analogue. The radiative rate constant is described as

$$k_r = \frac{\Phi_f}{\tau_f} \quad (4)$$

Here, τ_f and Φ_f signifies lifetime and quantum yield of the compound respectively.

Calculation of change in free energy (ΔG): The change in Gibbs free energy during the adduct formation between the probes and BSA was measured by subsequent equation [3]

$$\Delta G = -2.303RT\log K_a$$

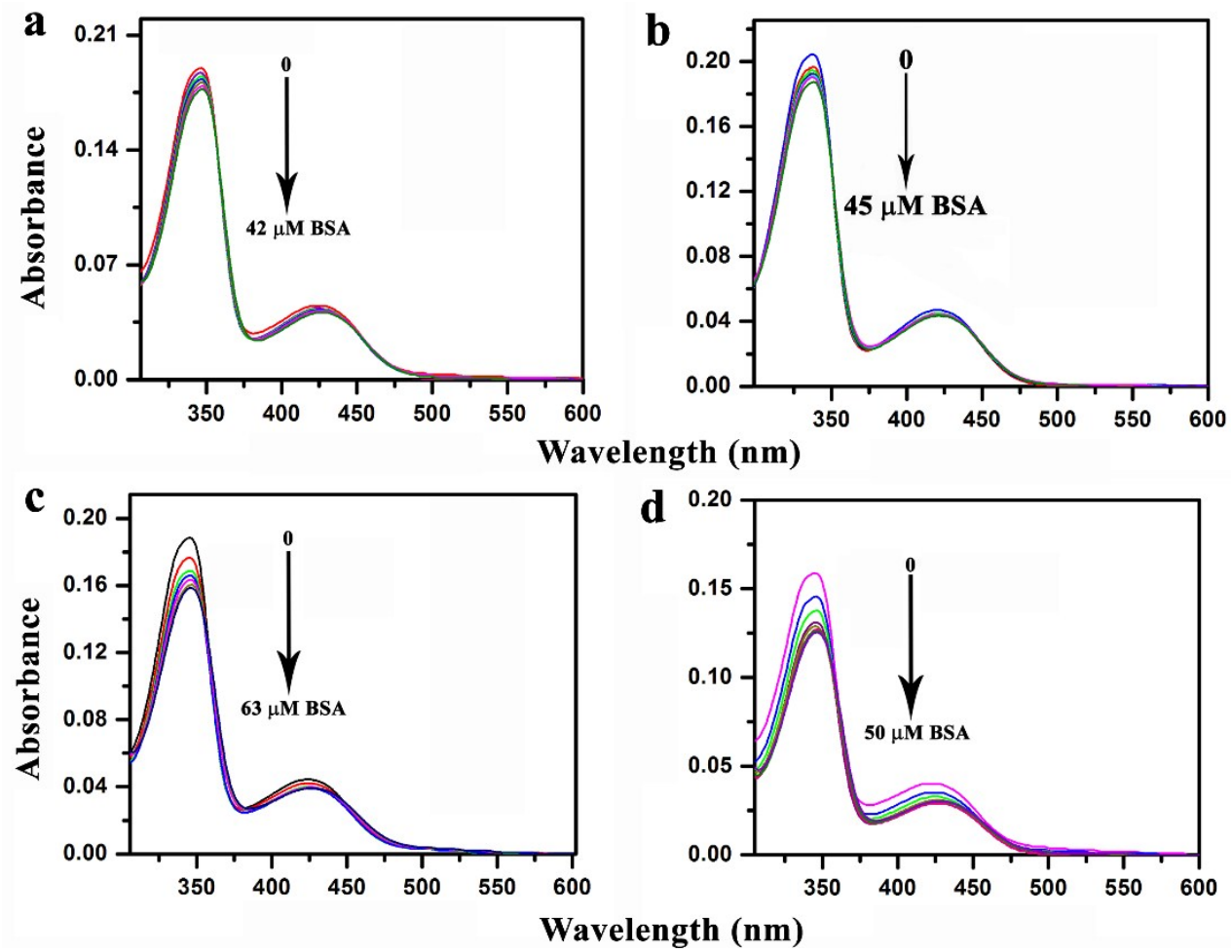

Fig. S1 Absorption spectra of berberine analogues (5 μM) with increasing concentrations of BSA in CP buffer of pH 7.1, (a) BZ_1, (b) BZ_2, (c) BZ_3, (d) BZ_5.

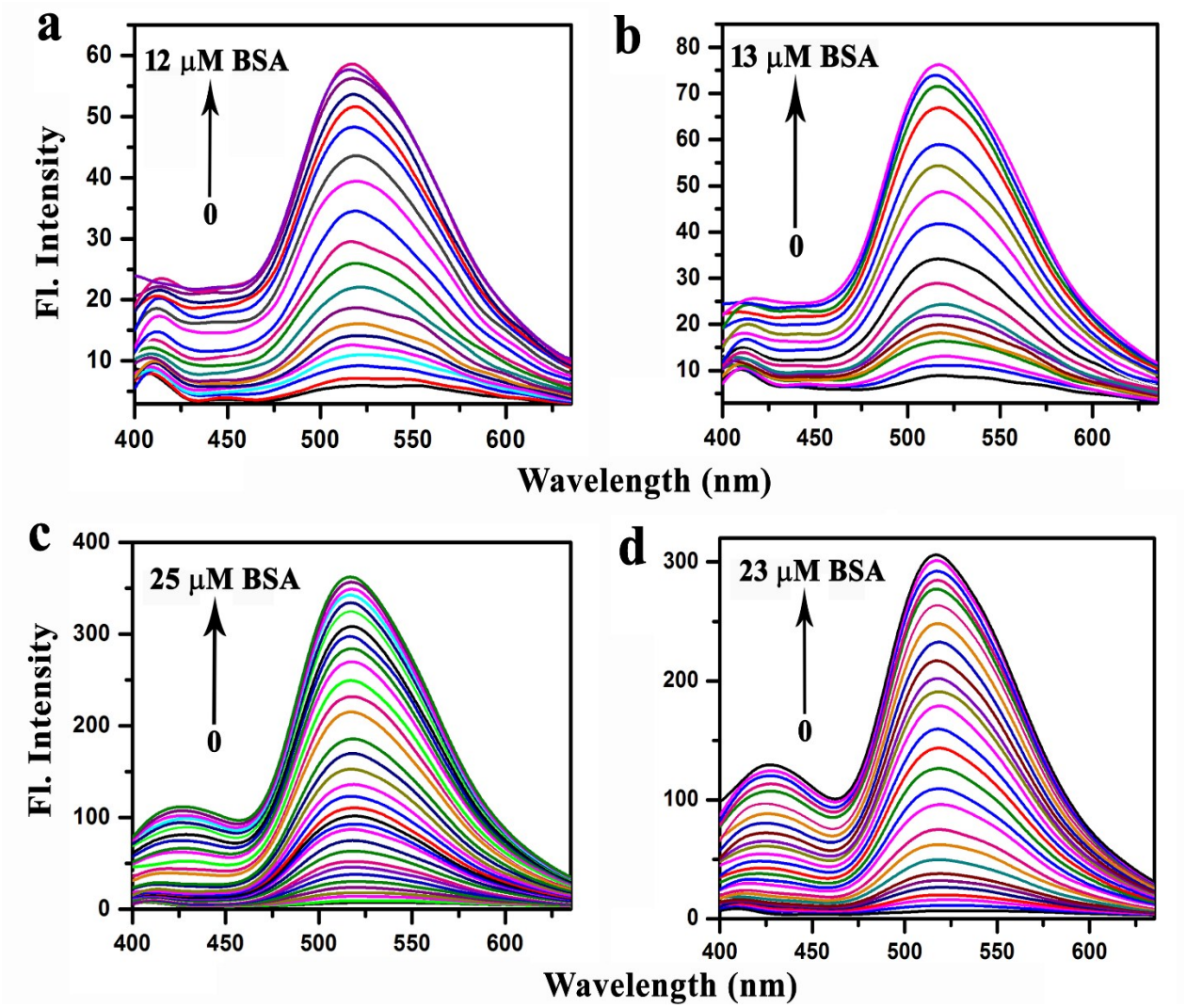

Fig. S2 Fluorescence titration spectra of Synthesized berberine analogues (5 μM), (a) BZ_1, (b) BZ_2, (c) BZ_3, (d) BZ_5 with increasing concentration of BSA up to saturation in CP buffer solution (pH 7.2, 10 mM).

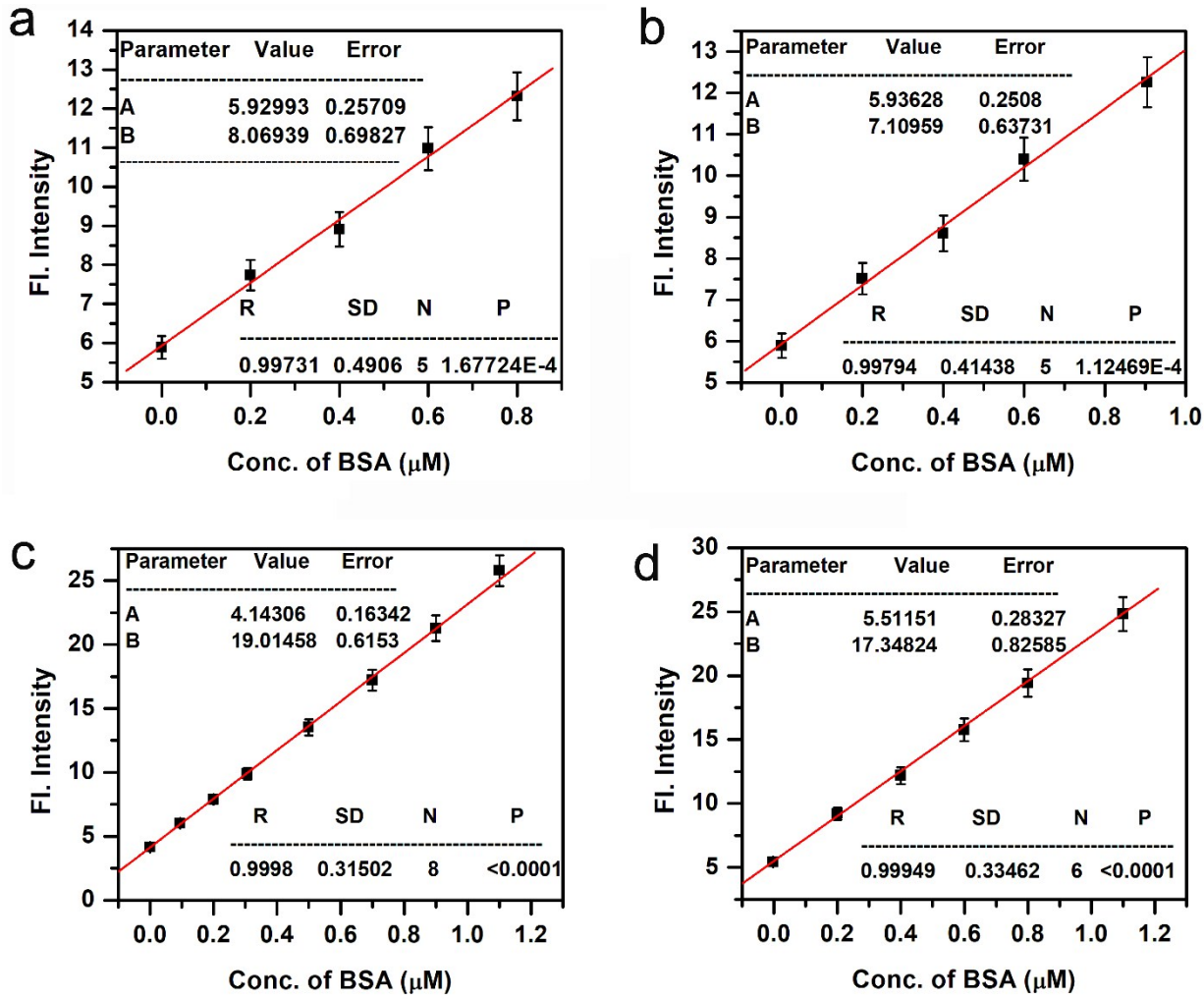

Fig. S3 The plot of fluorescence intensity of analogues with respect to addition of BSA in the linearity range, (a) BZ_1, (b) BZ_2, (c) BZ_3 and (d) BZ_5.

Table: S1 BSA binding constant (K_{BH}) of berberine analogues obtained from Benesi-Hildebrand plot	
Entry	K_{BH}
BZ_1	2.5×10^4
BZ_2	3.1×10^4
BZ_3	6.8×10^4
BZ_4	7.3×10^4
BZ_5	5.7×10^4

Table: S2 Comparative BSA sensing ability of synthesized berberine analogues		
Berberine analogues	Linearity range (μM)	LOD (μM)
BZ_1	0 –0.8	0.200
BZ_2	0 –0.9	0.192
BZ_3	0 –1.1	0.054
BZ_5	0 –1.1	0.063

Table: S3 Comparison of some published BSA sensor relating various critical aspects					
Probe	Solvent system	Method	Linear range	LOD	Reference
Dansylamide substituted probe (DNSA-SQ)	Phosphate buffer (10 mM, pH 7.2)	Fluorometric	0.5 – 3 equiv	1 μg/ml	33
Graphene oxide based biosensor	……	Fluorometric	0 –60 μg/ml	0.4 μM	28
Hydroxylated carbazole	PBS (pH 7.4, 10X)	Fluorometric	0 –1 μM	5 nM	3
5-(alkoxy) naphthalene	Aqueous buffer (pH 7.0)	Fluorometric	0 – 275 μg/ml	....	45
BDAZn-GO	Water-ethanol (1:1)	Fluorometric	0.714 – 1.25 mg/ml	0.0715 mg/ml	30
FPI based NIR probe	PBS buffer+ DMSO	Fluorometric	0-4 μM	30 nM	31
Berberine analogue (BZ_4)	CP buffer	Fluorometric	0– 2.5 μM	3.3 nM	This work

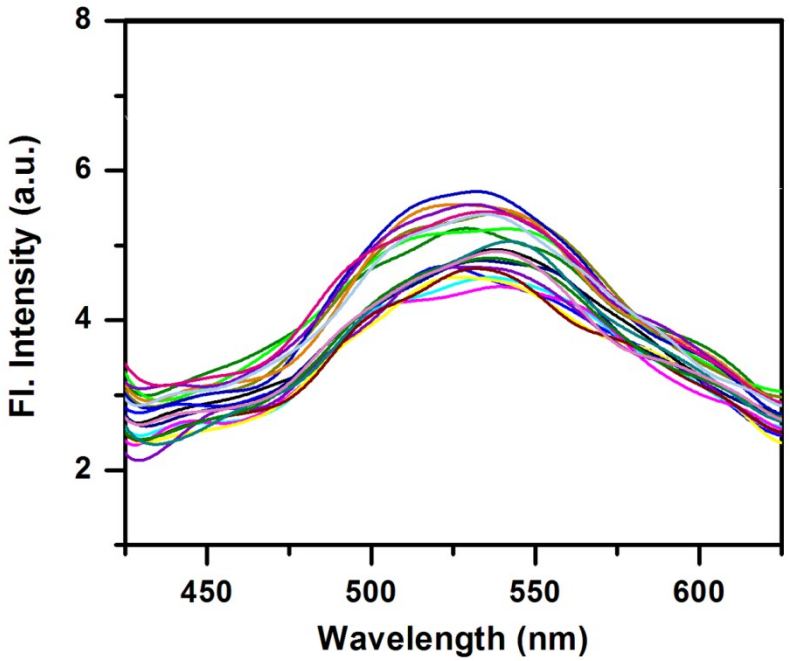

Fig. S4 Emission spectra of BZ_4 (5 μM) recorded in the presence of various anions, F^- Cl^-, Br^-, I^-, CO_3^{2-}, SO_4^{2-}, HPO_4^{2-}, SCN^-, CO_3^{2-}, BO_3^{3-}, NO_2^-, NO_3^-, S^{2-}, $HCO3^-$, HPO_4^-, SO_3^{2-}, $B_4O_7^{2-}$, $S_2O_3^{2-}$).

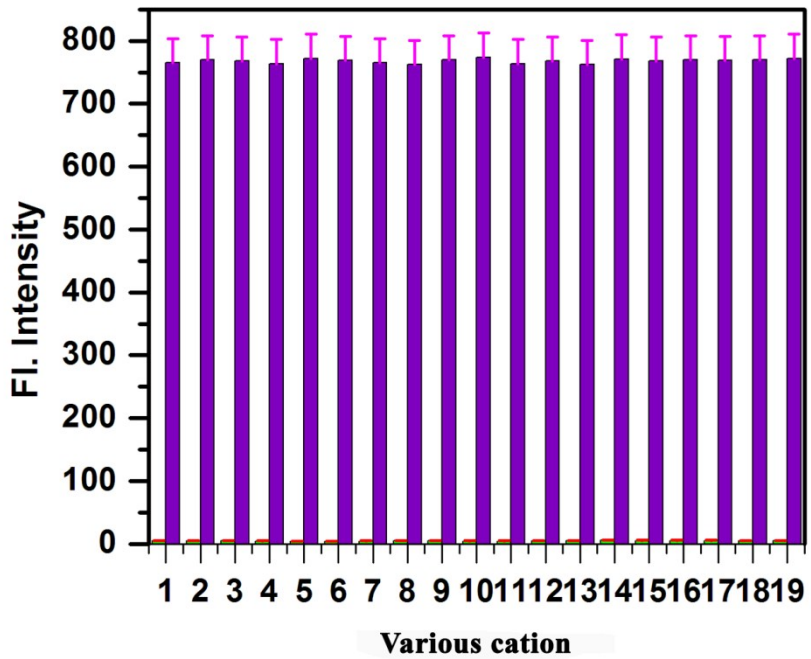

Fig. S5 Interfering effects to various anions in CP buffer (10 mM, pH 7.2). The green bars represent the intensity of BZ_4 in the presence of anions (each of 28 μM). The violet bars signify the changes of the ratios that occurs upon the consequent addition of 28 μM of BSA to the above solution.

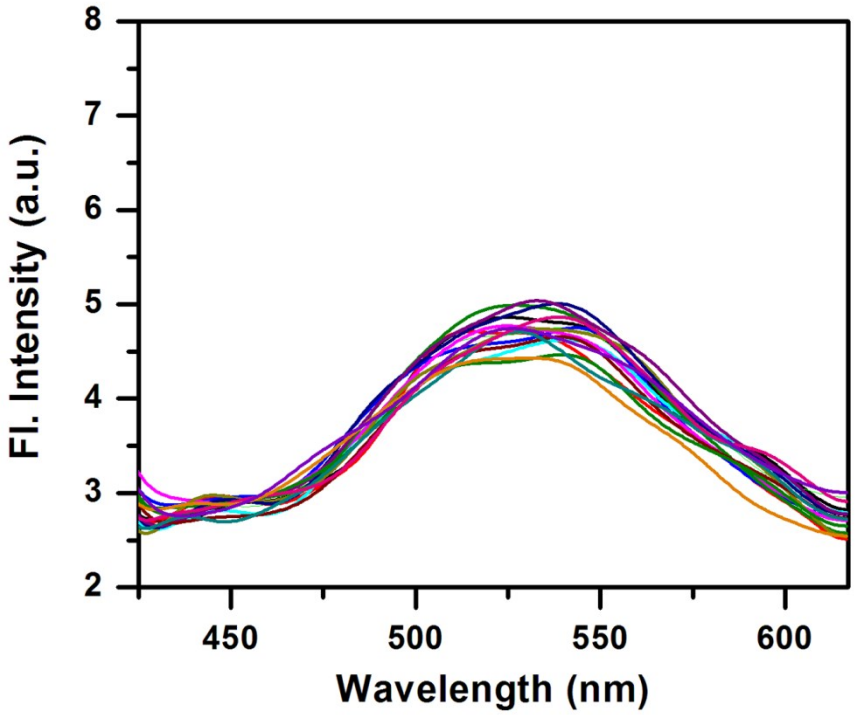

Fig. S6 Emission spectra of BZ_4 (5 μM) recorded in the presence of various cations (28 μM each, Na^+, K^+, Au^+, Ag^+, Ni^{2+}, Mg^{2+}, Ca^{2+}, Cu^{2+}, Cd^{2+}, Hg^{2+}, Pb^{2+}, Fe^{2+}, Al^{3+}, Zn^{2+}, Sr^{2+}).

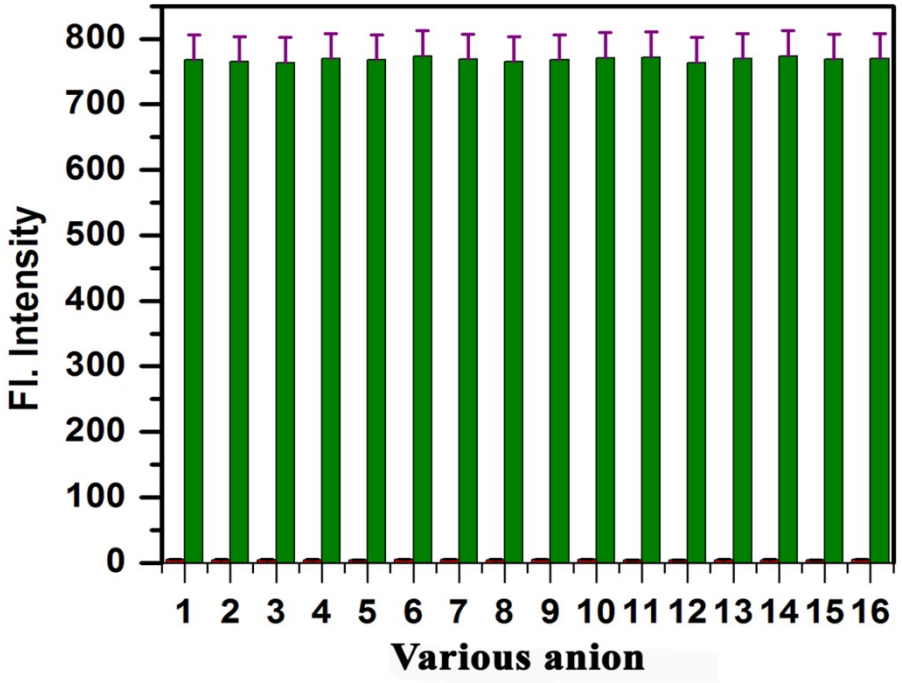

Fig. S7 Interfering effects to various anions in CP buffer (10 mM, pH = 7.2). The green bars represent the intensity of BZ_4 in the presence of cations (each of 28 μM). The green bars signify the changes of the ratios that occurs upon the consequent addition of 28 μM of BSA to the above solution.

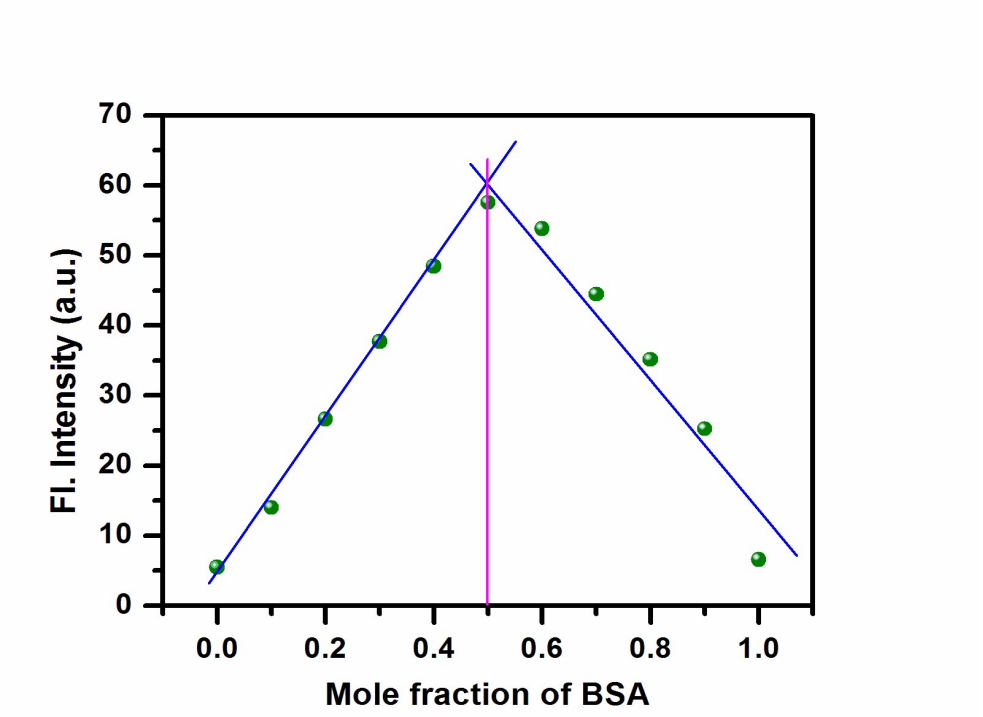

Fig. S8 The emission intensity of the solution containing BZ_4 and BSA varying concentration of both but keeping total concentration 5 μM.

.

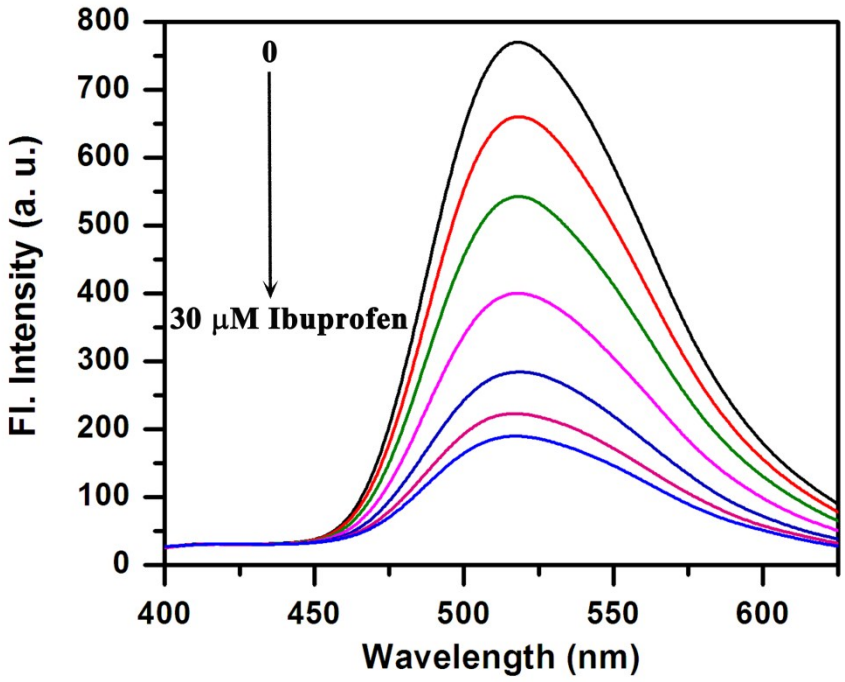

Fig. S9 The variation of fluorescence intensity of BZ_4 + BSA (5μM + 28 μM) upon addition of site marker, ibuprofen.

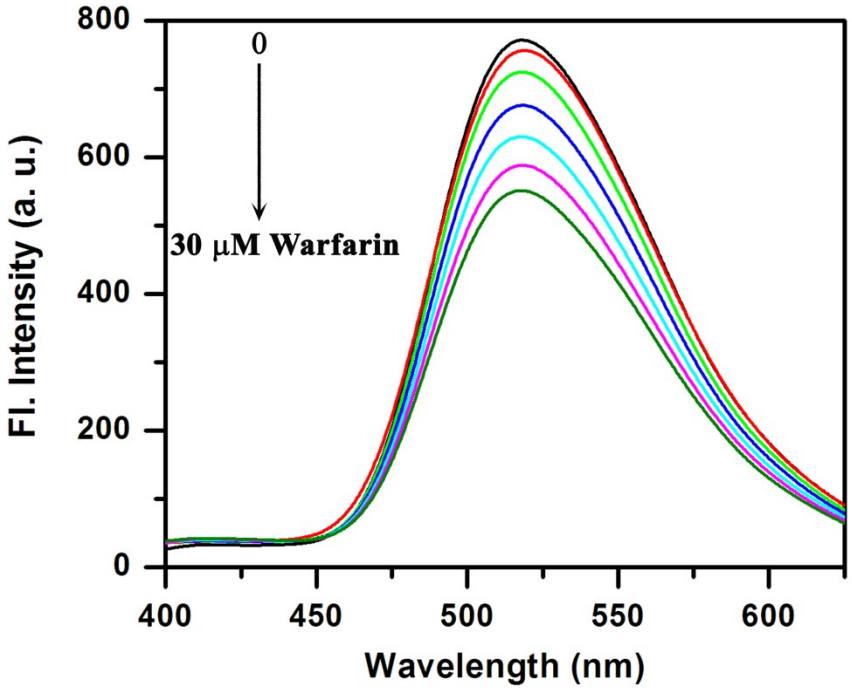

Fig. S10 The variation of fluorescence intensity of BZ_4 + BSA (5μM + 28 μM) upon addition of site marker, warfarin.

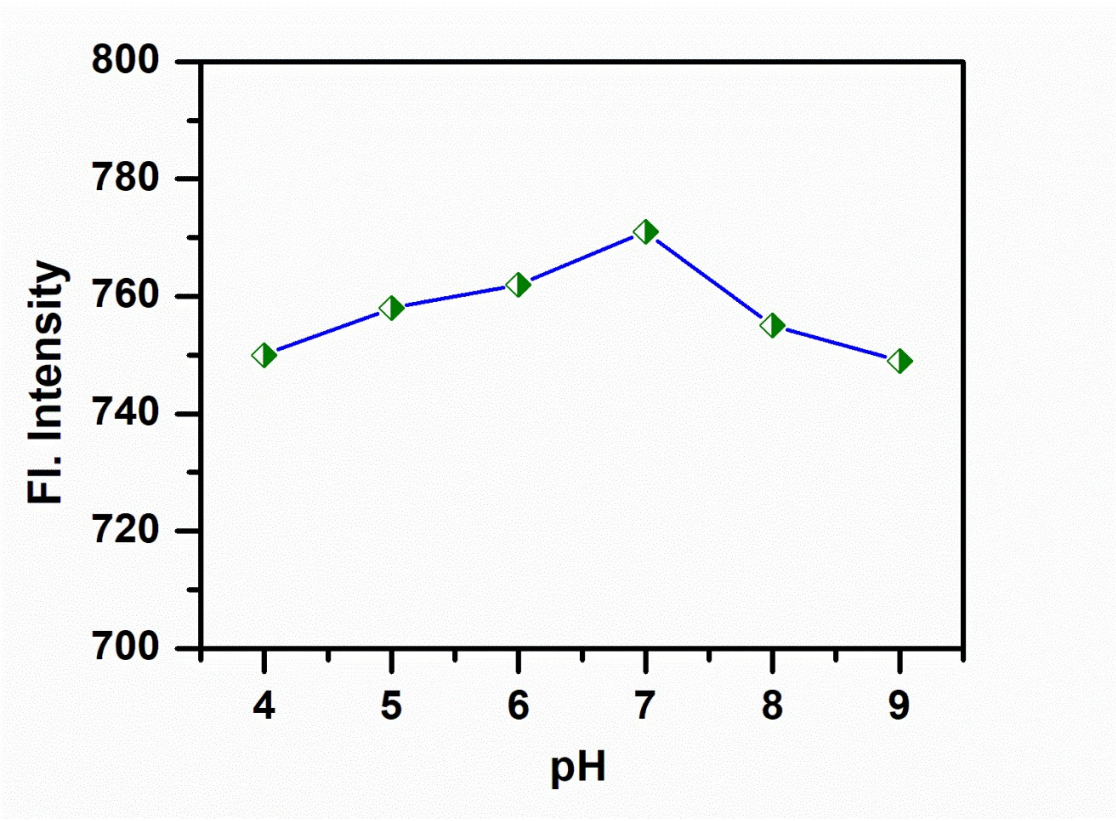

Fig. S11 The effect of pH on interaction of BZ4 with BSA, where BZ_4+BSA (5 μM+28 μM).

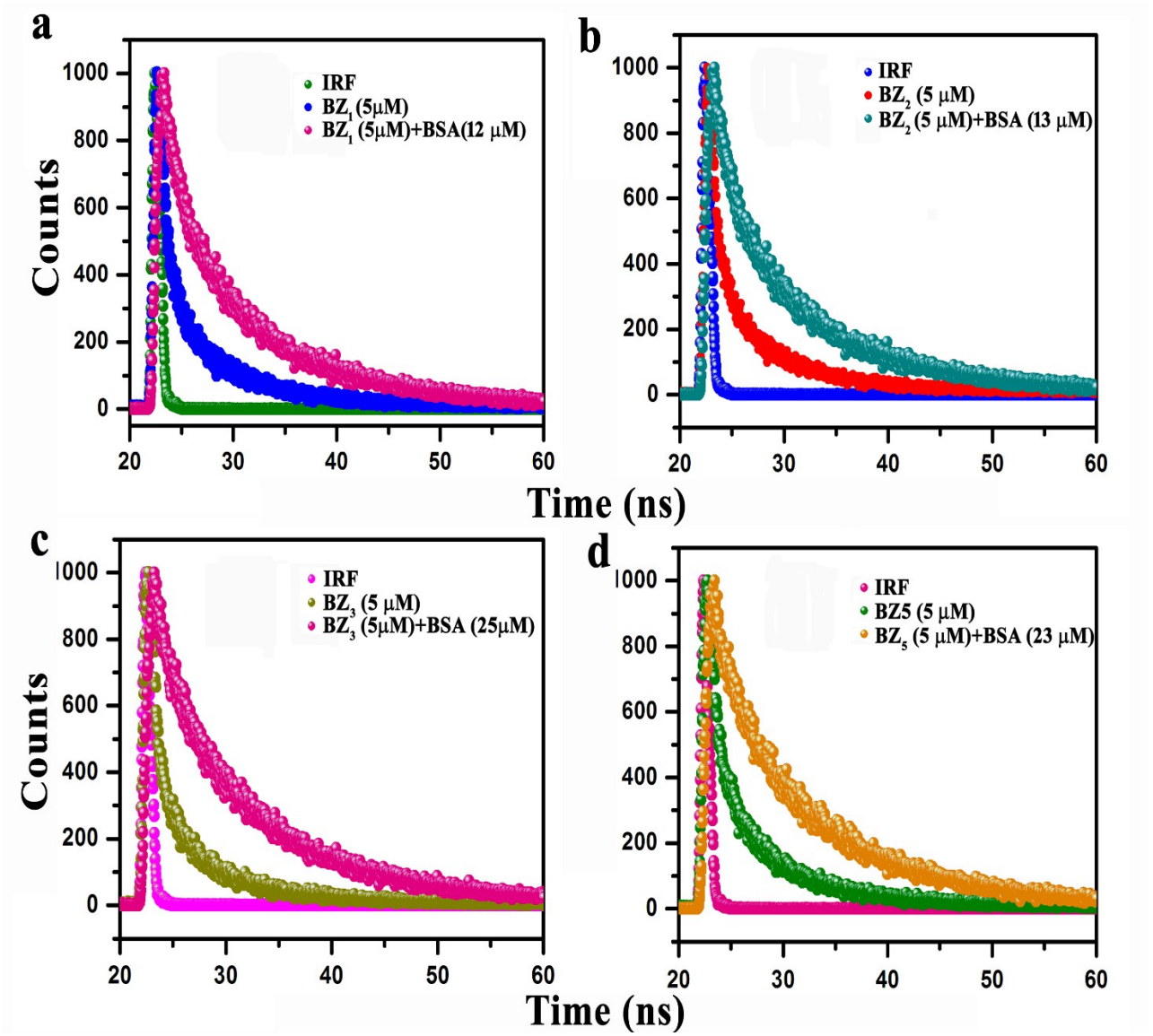

Fig. S12 Time resolved fluorescence spectra of the compounds (a) BZ_1, (b) BZ_2, (c) BZ_3 and (d) BZ_5 (5 μM) in absence and in presence of BSA in CP buffer (pH 7.2, 10mM).

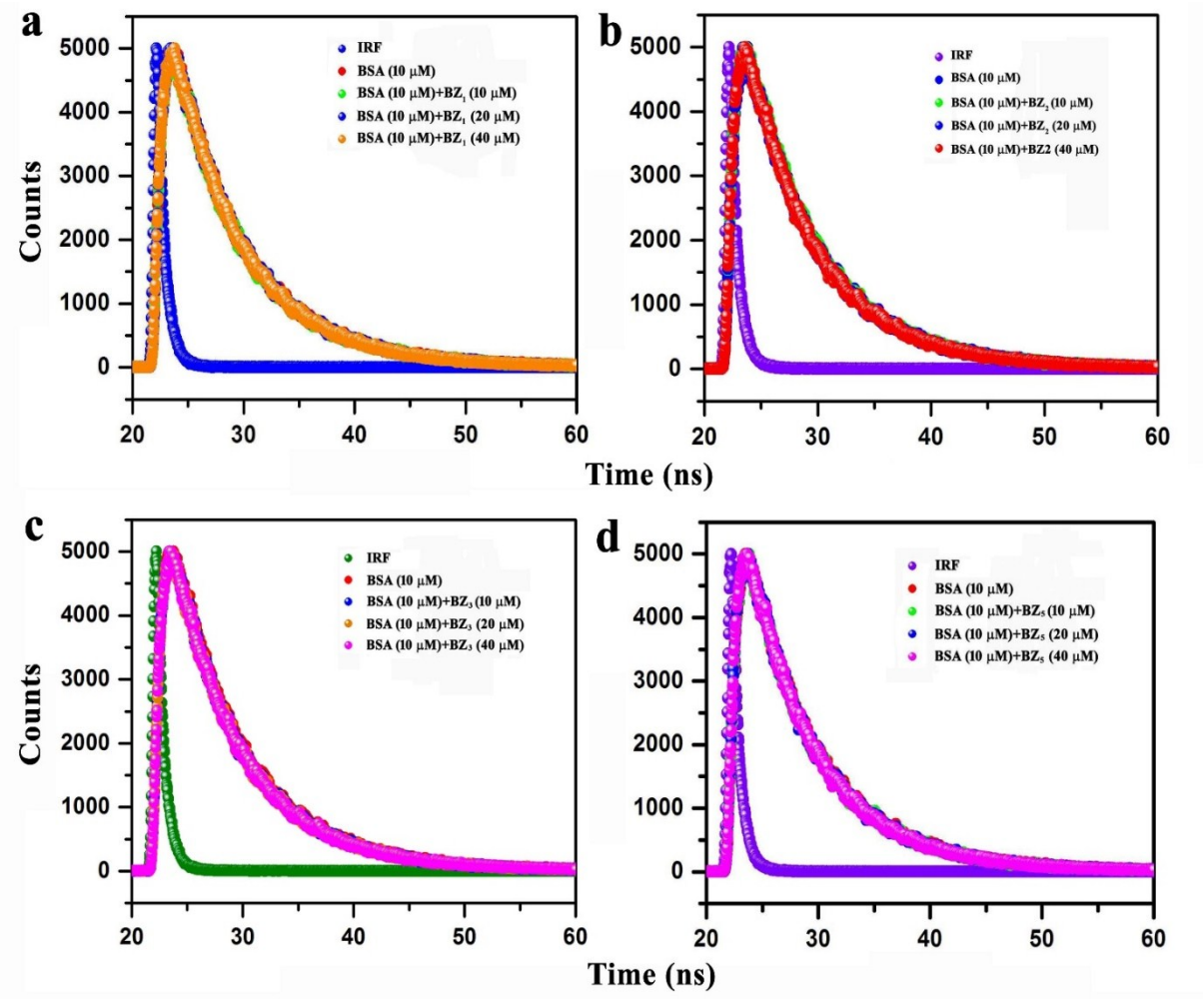

Fig. S13 Lifetime decay profile of BSA (10 μM) in presence of different concentration of probes, (a) BZ_1, (b) BZ_2, (c) BZ_3 and (d) BZ_5.

Table: S4 Lifetime of BSA in presence of synthesized analogues.								
Entry	τ_1 (ns)	α_1	τ_2 (ns)	α_2	τ_3 (ns)	α_3	τ_m	$\chi 2$
Native BSA	2.03	0.09	4.79	0.45	7.66	0.46	5.86	1.04
BSA + 10 μM BZ_1	3.64	0.28	7.14	0.67	8.54	0.05	6.23	1.07
BSA + 20 μM BZ_1	2.86	0.18	6.56	0.81	20.9	0.01	6.03	1.08
BSA + 40 μM BZ_1	3.19	0.23	6.72	0.77	-	-	5.90	1.09
BSA + 10 μM BZ_2	2.88	0.17	5.6	0.42	7.42	0.41	5.88	1.05
BSA + 20 μM BZ_2	2.51	0.15	6.17	0.78	10.2	0.07	5.90	1.02
BSA + 40 μM BZ_2	1.22	0.03	3.54	0.28	6.88	0.69	5.77	1.03
BSA + 10 μM BZ_3	3.38	0.30	6.92	0.70	-	-	5.85	1.05
BSA + 20 μM BZ_3	3.14	0.28	6.88	0.72	-	-	5.83	1.01
BSA + 40 μM BZ_3	3.59	0.34	7.03	0.66	-	-	5.86	1.09
BSA + 10 μM BZ_4	1.2	0.07	3.71	0.29	7.06	0.64	5.67	1.04
BSA + 20 μM BZ_4	1.32	0.11	5.04	0.57	8.13	0.32	5.62	1.03
BSA + 40 μM BZ_4	1.13	0.11	4.26	0.36	7.23	0.53	5.48	1.05
BSA + 10 μM BZ_5	2.15	0.12	5.42	0.59	8.13	0.29	5.81	1.02
BSA + 20 μM BZ_5	1.8	0.10	5.15	0.55	7.88	0.35	5.77	1.05
BSA + 40 μM BZ_5	1.32	0.06	3.63	0.28	6.88	0.67	5.70	1.06

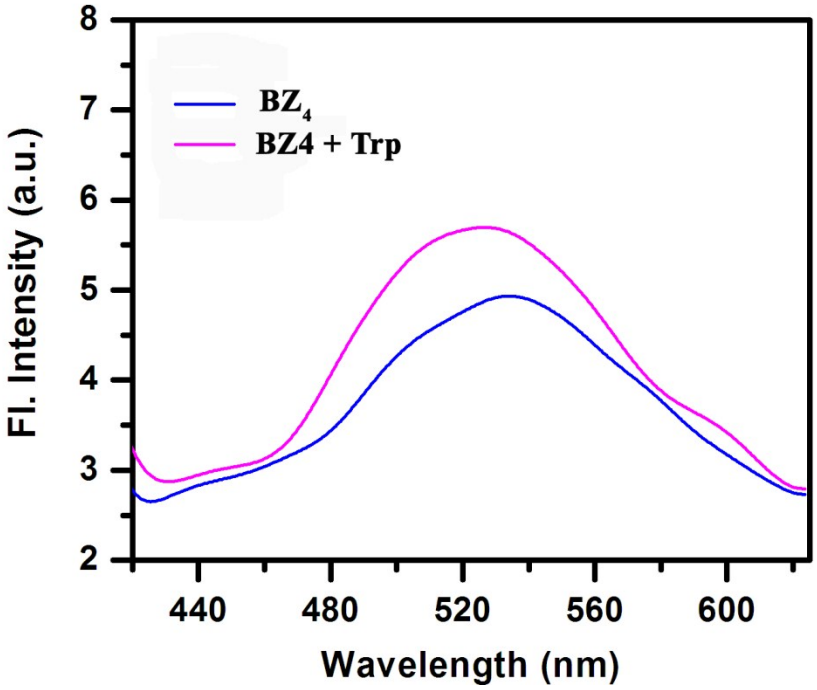

Fig. S14 The fluorescence response of BZ_4 (5 μM) upon addition of 28 μM tryptophan solution

Table: S5 3D fluorescence spectral data analysis

Entry	Peak1(λex/λem)	Stokes shift (Δλ=λem – λex)	Intensity	Peak2(λex/λem)	Stokes shift (Δλ=λem – λex)	Intensity
BSA	280/345	65	895	230/345	115	989
BSA+BZ_1	280/362	82	600	230/359	129	628
BSA+BZ_2	280/363	83	497	230/360	130	537
BSA+BZ_3	280/364	84	416	230/363	133	509
BSA+BZ_4	280/364	84	477	230/364	134	467
BSA+BZ_5	280/364	84	486	230/361	131	518

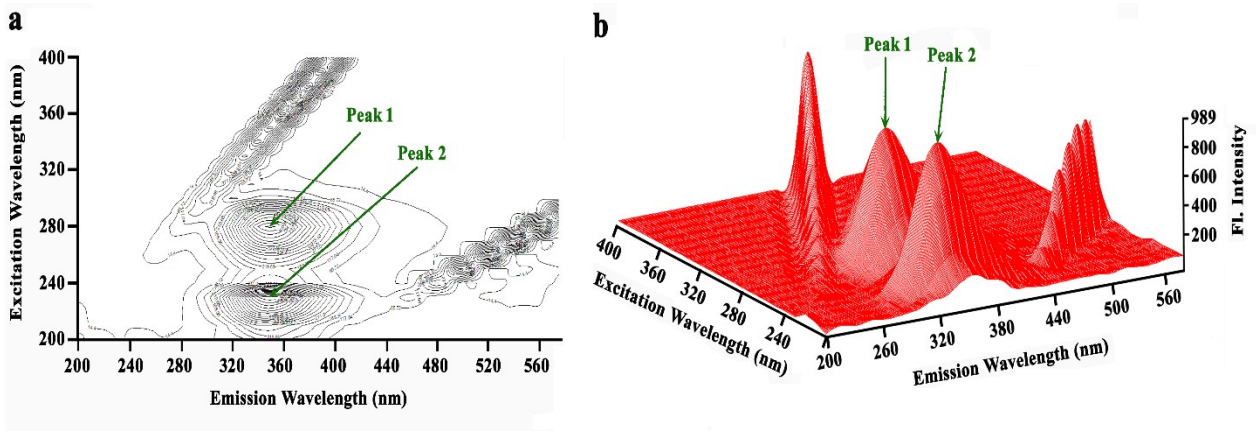

Fig. S15 3D fluorescence spectra of BSA with varying excitation and emission wavelength (a) contour projection and (b) surface projection.

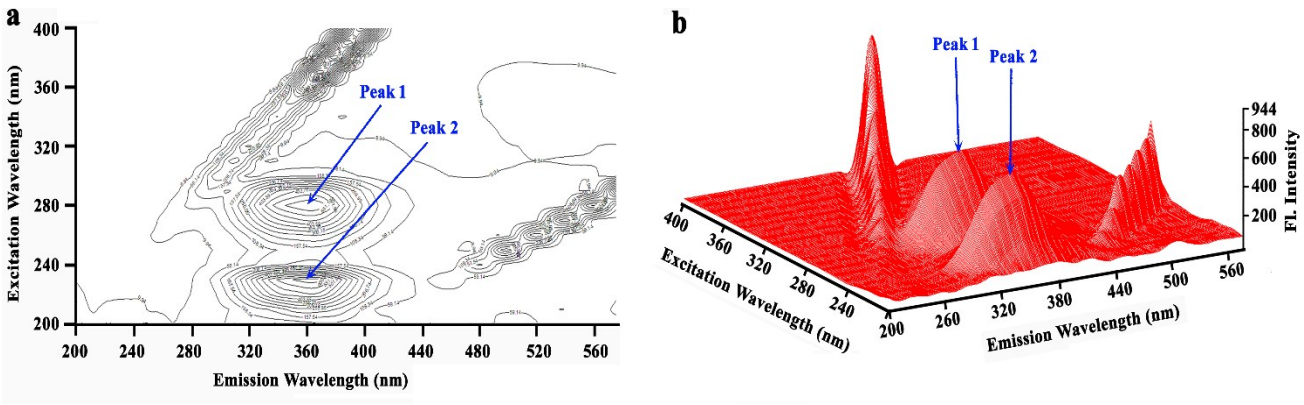

Fig. S16 3D fluorescence spectra of BSA + BZ_1 complex with varying excitation and emission wavelength (a) contour projection and (b) surface projection.

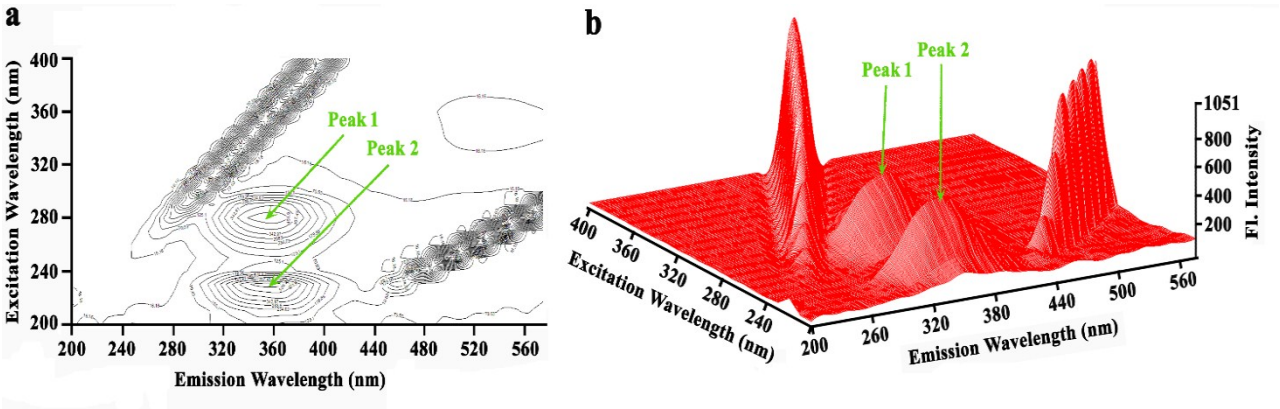

Fig. S17 3D fluorescence spectra of BSA + BZ_2 complex with varying excitation and emission wavelength (a) contour projection and (b) surface projection.

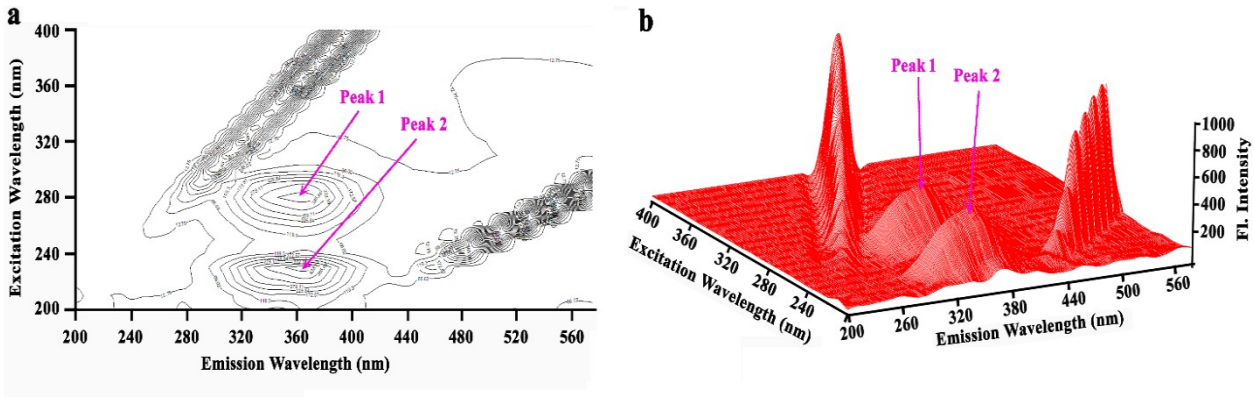

Fig. S18 3D fluorescence spectra of BSA + BZ_3 complex with varying excitation and emission wavelength (a) contour projection and (b) surface projection.

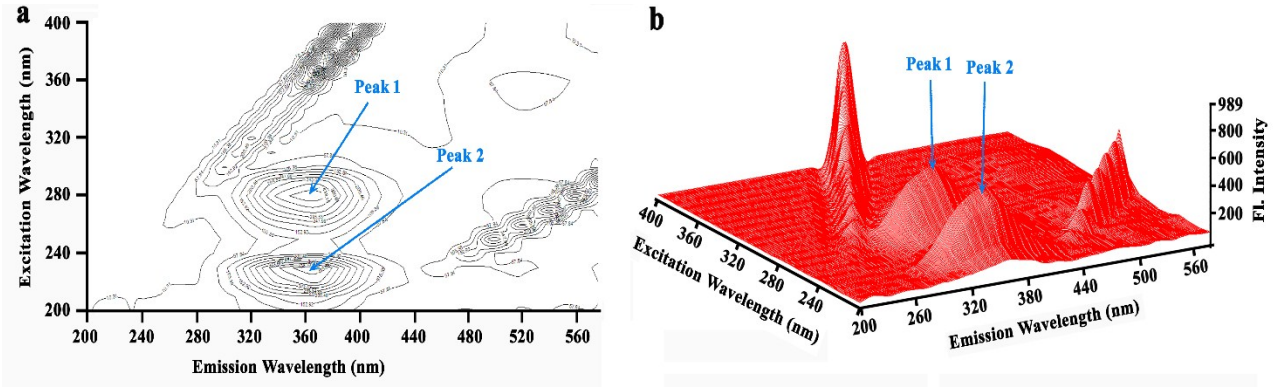

Fig. S19 3D fluorescence spectra of BSA + BZ_4 complex with varying excitation and emission wavelength (a) contour projection and (b) surface projection.

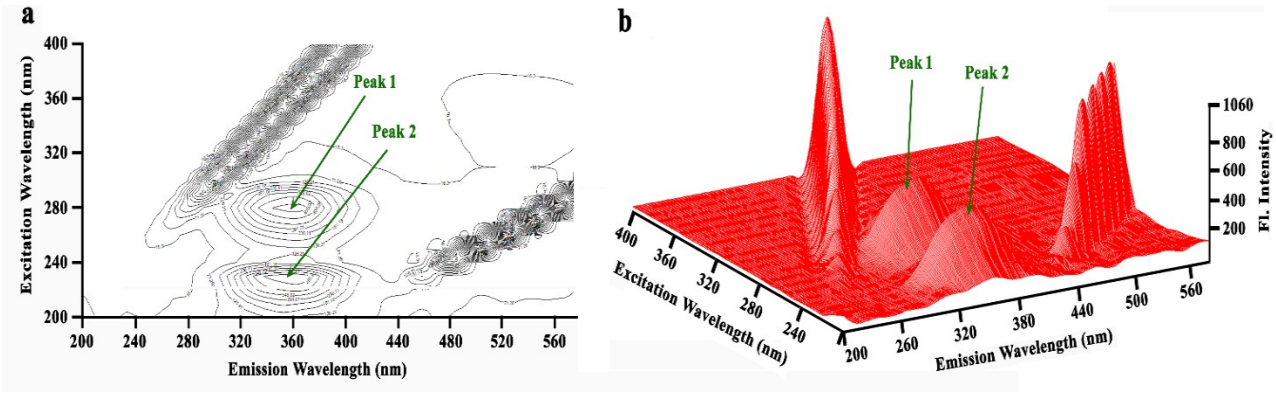

Fig. S20 3D fluorescence spectra of BSA + BZ_5 complex with varying excitation and emission wavelength (a) contour projection and (b) surface projection.

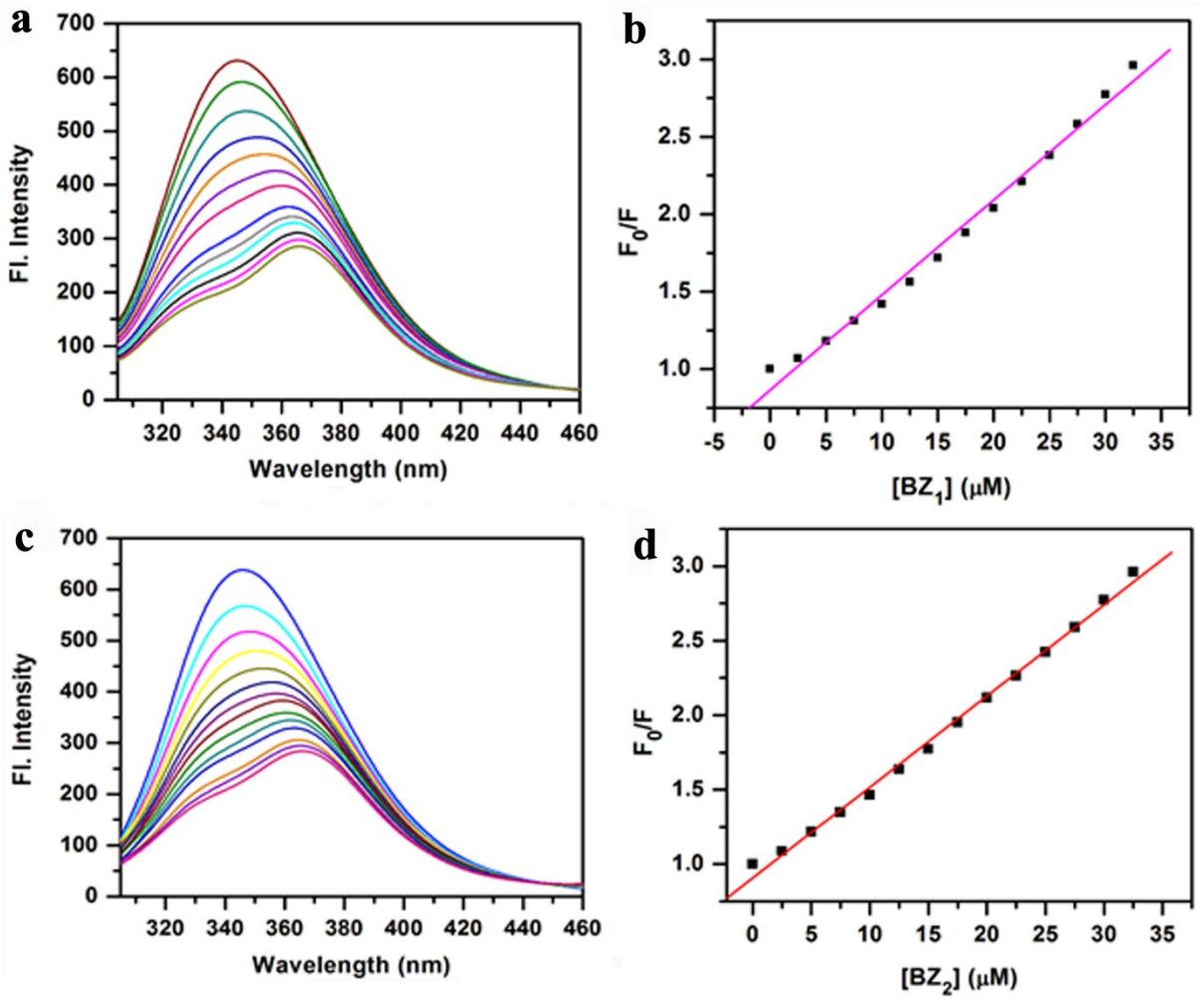

Fig. S21 (A) Fluorescence spectra of 5 μM BSA in the presence of increasing concentrations of probe (a) BZ_1 and (c) BZ_2 in the range from 0 to 40 μM at pH 7.2 in 10 mM CP buffer, (B) respective Stern-Volmer plots of the BSA-ligand complex (F_0/F versus concentration of BZ_1 and BZ_2).

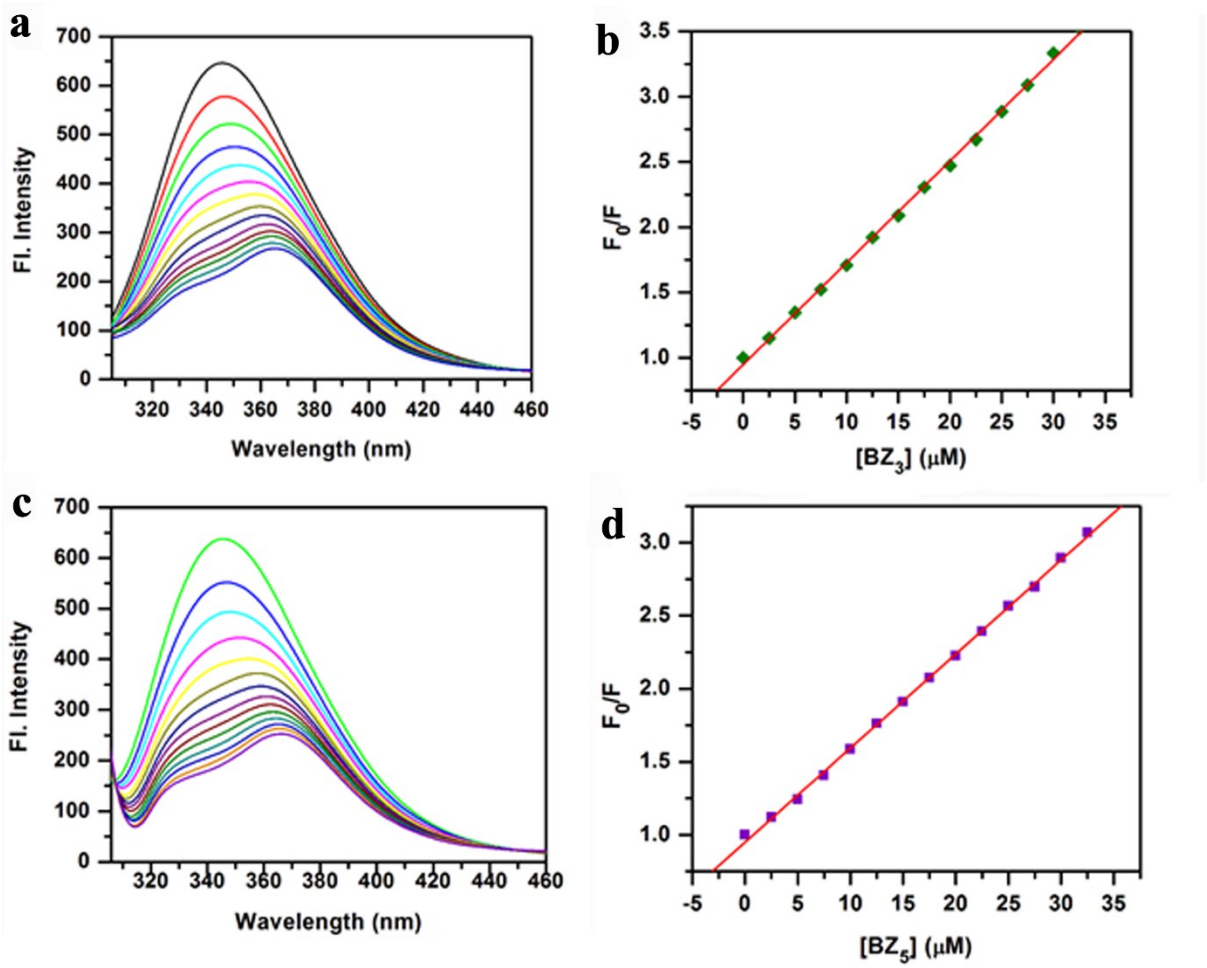

Fig. S22 (A) Fluorescence spectra of 5 μM BSA in the presence of increasing concentrations of probe (a) BZ_3 and (c) BZ_5 in the range from 0 to 40 μM at pH 7.2 in 10 mM CP buffer, (B) respective Stern-Volmer plots of the BSA-ligand complex (F_0/F versus concentration of BZ_3 and BZ_5).

Table: S6 Quenching parameter for various BSA- berberine analogue complexes			
Entry	K_{sv}[a] (M^{-1})	K_A[b] (M^{-1})	n[c]
BSA + BZ_1	4.66×10^4	2.2×10^4	1.05
BSA + BZ_2	5.98×10^4	3.1×10^4	1.08
BSA + BZ_3	12.85×10^4	5.2×10^4	1.06
BSA + BZ_4	17.47×10^4	5.6×10^4	1.04
BSA + BZ_5	12.04×10^4	4.3×10^4	1.07

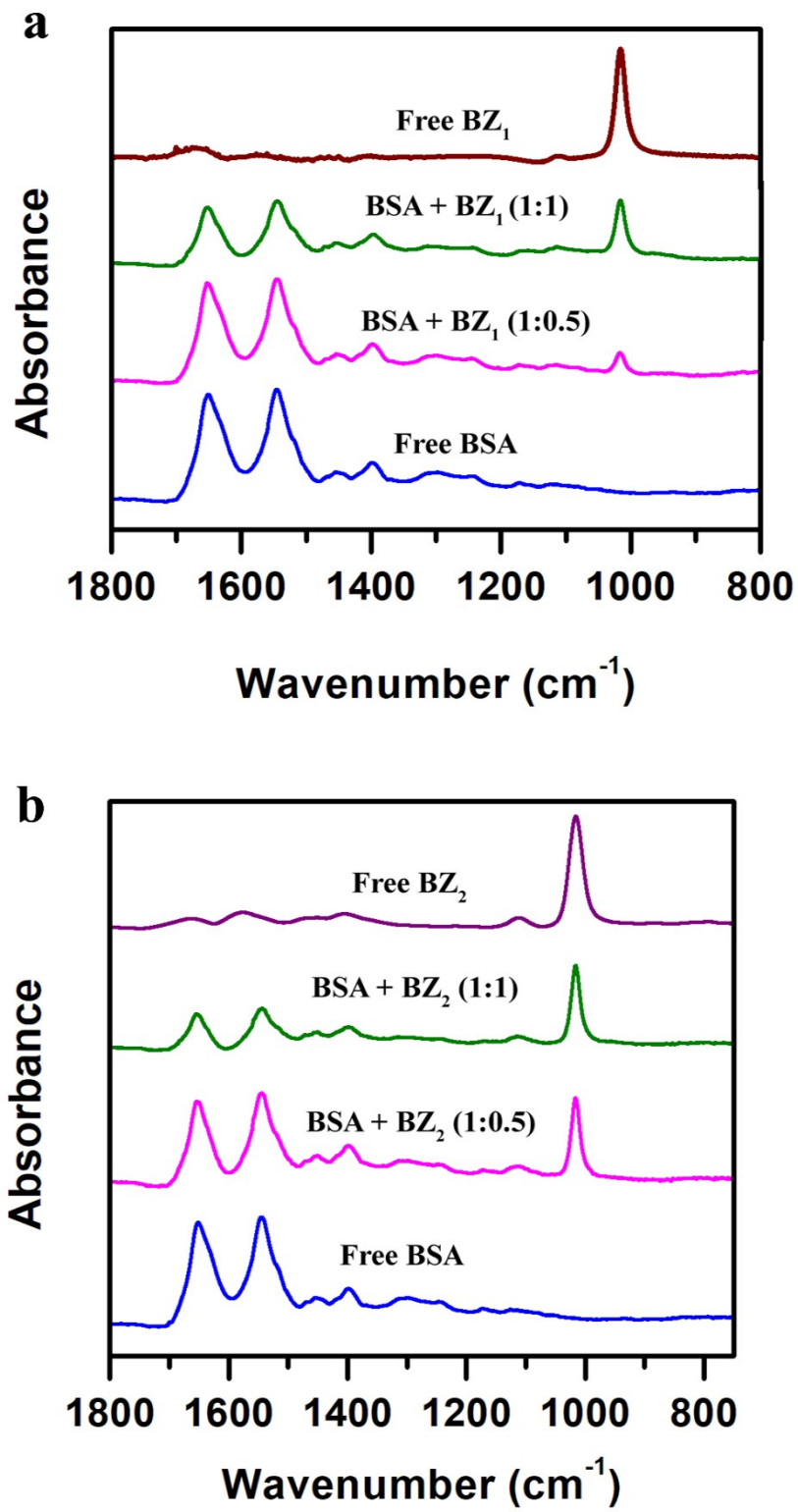

Fig. S23 FT-IR spectra in the region of 1800 to 800 cm^{-1} of hydrated films (at pH 7.2 in 10 mM [Na+] CP buffer, 25°C) for (a) free BSA and its complex (BSA+BZ_1) at different concentrations, (b) free BSA and its complex (BSA+BZ_2) at different concentrations.

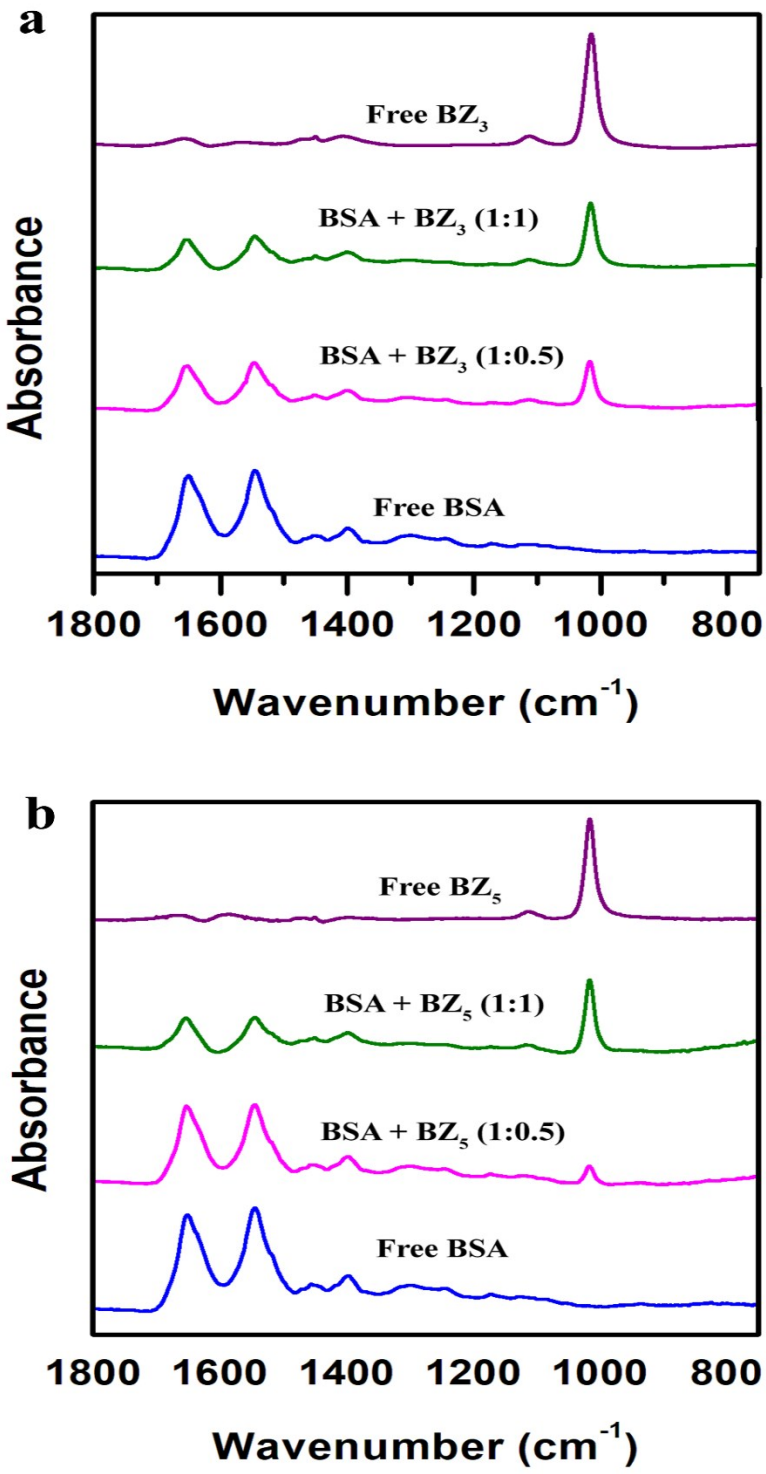

Fig. S24 FT-IR spectra in the region of 1800 to 800 cm^{-1} of hydrated films (at pH 7.2 in 10 mM [Na+] CP buffer, 25°C) for (a) free BSA and its complex (BSA+BZ_3) at different concentrations, (b) free BSA and its complex (BSA+BZ_5) at different concentrations.

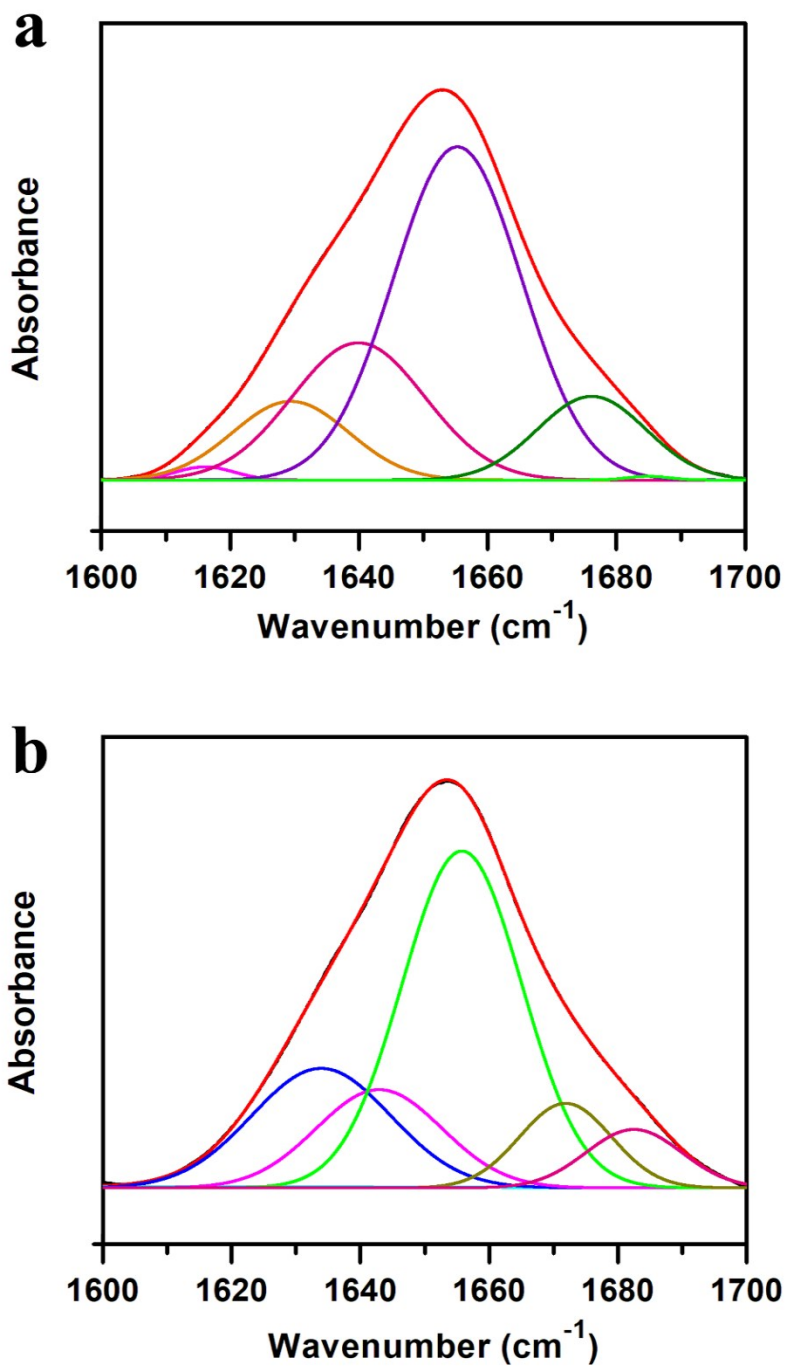

Fig. S25 Second derivative resolution enhancement and curve-fitted amide I region (1700-1600cm−1) for (a) BSA-BZ_1 complex and (b) BSA-BZ_2 complex.

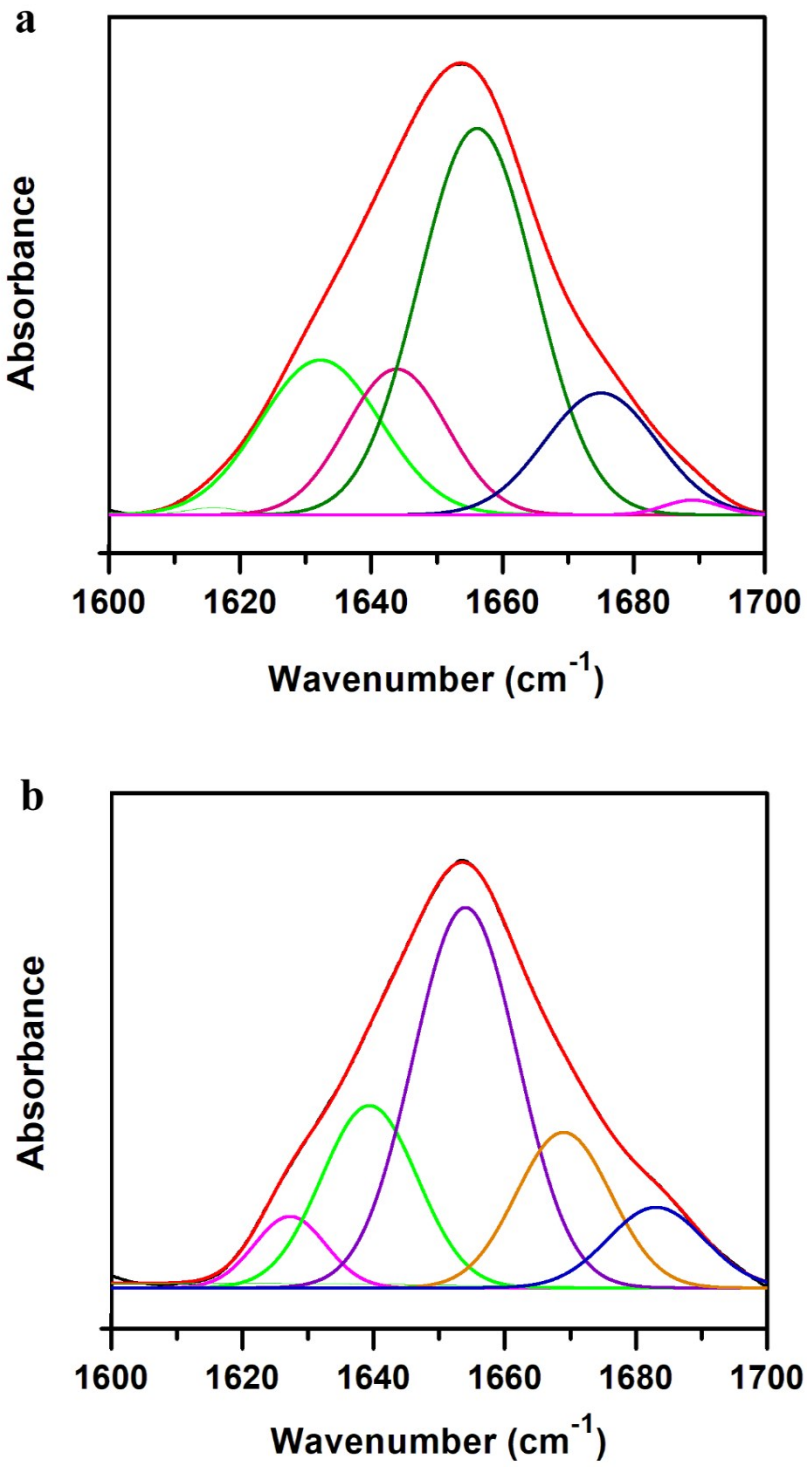

Fig. S26 Second derivative resolution enhancement and curve-fitted amide I region (1700-1600cm−1) for (a) BSA-BZ_3 complex and (b) BSA-BZ_5 complex.

Table: S7 Analysis of secondary structure of free BSA and BSA-berberine analogues composite at pH 7.2 from FT-IR						
Amide I components (cm^{-1})	Free BSA	BSA-BZ_1(1:1)	BSA-BZ_2(1:1)	BSA-BZ_3(1:1)	BSA-BZ_4(1:1)	BSA-BZ_5(1:1)
β-anti (1692–1680) (±1%)	4	1	7	1	5	7
Turn (1680–1660) (±1%)	4	12	10	13	9	11
α-helix (1660–1650) (±2%)	55	53	50	49	46	47
Random coil (1648–1641) (±1%)	10	22	16	17	28	20
β-sheet (1640–1610) (±2%)	27	12	17	20	12	12
An average of three determination.						

Table: S8 Molecular docking data			
ΔG	rmsd	ΔG conf	ΔG place
-10.425905	9.2527704	3.8795543	-596.97272
-9.4489584	9.1353407	3.6653197	-607.06976
-9.6691275	9.1338263	3.2104187	-645.56812
-9.7326403	9.1166897	3.8261092	-564.95605
-9.460638	9.0859594	3.8224683	-569.94495
-9.5036402	9.0219431	2.8695779	-585.07037
-9.5424271	8.8645029	3.7385738	-552.72961
-10.428071	8.5361052	3.6117456	-617.17285
-9.6163368	8.2454977	3.2166734	-577.81647

-9.3277645	8.2444773	3.8058341	-585.25269
-10.752552	8.0968914	3.5999999	-586.26801
-10.771677	8.0766153	3.6159236	-567.97131
-10.484232	8.0504694	3.2159235	-565.67975
-10.685371	8.0410366	3.2	-558.83826
-9.9006023	7.7852068	2.5597858	-601.15149
-9.8945007	5.8259711	3.2844515	-571.46582
-10.913427	5.37427	2.4564912	-578.94708
-9.7262173	3.8846083	4.3047547	-616.93994
-10.035133	3.8233447	2.6454575	-608.02319
-9.5275078	3.7175879	3.6178336	-608.93042
-9.3883715	3.717176	4.3444934	-599.18323
-10.016923	3.6190224	3.3269715	-581.20648
-9.897151	3.5962861	2.7749085	-576.56659
-9.3826494	3.5864789	3.2087717	-598.49976
-9.780385	3.5614181	3.6144423	-576.2074
-9.4827108	3.5467737	2.6482136	-588.18158
-9.5212231	3.4504273	2.6278791	-580.32184
-9.3982248	3.1488724	3.9454179	-590.07153
-9.9747019	3.1448007	2.2057986	-554.6463
-9.3491564	2.9691839	2.2	-567.32068

Characterisation of berberine analogues (1-5):

BZ_1: 9-O-(benzyl) berberrubine (Yellowish solid, 66% yield):

^{1}H- NMR (400 MHz, d_6-DMSO): δ 3.20 (2H, t, J= 7.5 Hz), 4.08 (3H, s), 4.92 (2H, t, J= 7.5 Hz), 5.34 (2H, s), 6.15 (2H, s), 7.09 (1H, s), 7.44 (2H, d, J= 10 Hz), 7.56 (3H, m), 7.78 (1H, s), 8.02 (1H, d, J= 10 Hz), 8.21 (1H, d, J= 10 Hz), 8.92 (1H, s), 9.8 (1H, s).

^{13}C- NMR (100 MHz, d_6-DMSO):

δ 28.8, 56.1, 58.7, 75.4, 101.2, 103.5, 110.5, 111.7, 116.7, 120.8, 123.5, 127.1, 127.6, 128.9, 131.6, 130.8, 136.7, 141.3, 146.3, 146.6, 147.1, 148.7, 149.7, 151.8.

MALDI-MS: Calc. for $C_{26}H_{22}NO_4^+$ 421.15; found 412.16

BZ_2: 9-O-(2-chlorobenzyl) berberrubine (Yellowish solid, 60% yield):

^{1}H- NMR (400 MHz, d_6-DMSO): δ 3.18 (2H, t, J= 6 HZ), 4.02 (3H, s), 4.86 (2H, t, J= 9 HZ), 5.45 (2H, s), 6.15 (2H, s), 7.058 (1H, s), 7.67 9(1H, d, J= 12 HZ), 7.77 (1H, d, J= 12 HZ), 8.06 (1H, d, J= 12 HZ), 8.20 (1H, s), 8.78 (1H, s), 9.82 (1H, s).

^{13}C- NMR (100 MHz, d_6-DMSO):

δ 28.8, 56.1, 58.7, 67.4, 101.2, 103.5, 110.5, 111.7, 116.7, 120.8, 123.5, 127, 128.5, 129, 130. 7, 131.6, 130.8, 134, 141.3, 146.3, 146.6, 147.1, 148.7, 149.7, 151.8.

MALDI-MS: Calc. for $C_{26}H_{21}ClNO_4^+$ 446.12; found 446.24

BZ_3: 9-O-(3-chlorobenzyl) berberrubine (Yellowish solid, 62% yield):

^{1}H- NMR (400 MHz, d_6-DMSO): δ 3.20 (2H, t, J= 6 HZ), 4.08 (3H, s), 4.92 (2H, t, J= 9 HZ), 5.34 (2H, s), 6.17 (2H, s), 7.09 (1H, s), 7.44 (1H, d, J= 12 HZ), (2H, m), 7.71 (1H, s), 7.78 (1H, s), 8.04 (1H, d, J= 12 HZ), 8.21 (1H, d, J= 12 HZ), 8.92 (1H, s), 9.80 (1H, s).

^{13}C- NMR (100 MHz, d_6-DMSO):

δ 28.8, 56.1, 58.7, 70.9, 101.2, 103.5, 110.5, 111.7, 116.7, 120.8, 123.5, 125.2, 126.9, 127.7, 130.3, 130.8, 131.6, 134.5, 141.3, 142.6, 146.3, 146.6, 147.1, 148.7, 149.7, 151.8.

MALDI-MS: Calc. for $C_{26}H_{21}ClNO_4^+$ 446.12; found 446.25

BZ_4: 9-O-(4-chlorobenzyl) berberrubine (Yellowish solid, 65% yield):

^{1}H- NMR (400 MHz, d_6-DMSO): δ 3.19 (2H, t, J= 10 HZ), 4.04 (3H, s), 4.90 (2H, t, J= 7.5 HZ), 5.40 (2H, s), 6.16 (2H, s), 7.08 (1H, s), 7.51 (1H, d, J= 5 HZ), 7.56 (2H, d, J= 10 HZ), 7.78 (1H, s), 8.07 (1H, d, J= 10 HZ), 8.21 (1H, d, J= 10 HZ), 8.92 (1H, s), 9.78 (1H, s).

^{13}C- NMR (100 MHz, d_6-DMSO):

δ 28.8, 56.1, 58.7, 75.4, 101.2, 103.5, 110.5, 111.7, 116.7, 120.8, 123.5, 129.0, 129.7, 130.8, 131.6, 133.2, 134.8, 141.3, 146.3, 146.6, 147.1, 148.7, 149.7, 151.8.

MALDI-MS: Calc. for $C_{26}H_{21}ClNO_4^+$ 446.12; found 446.15

BZ_5: 9-O-(2, 5-dichlorobenzyl) berberrubine (Yellowish solid, 58% yield):

^{1}H- NMR (400 MHz, d_6-DMSO): δ 3.19 (2H, t, J= 12 HZ), 4.04 (3H, s), 4.90 (2H, t, J= 9 HZ), 5.40 (2H, s), 6.16 (2H, s), 7.03 (1H, s), 7.33 (1H, d, J= 6 HZ), 7.51(1H, s), 7.72 (1H, d, J= 6 HZ), 7.78 (1H, s), 8.07 (1H, d, J= 12 HZ), 8.21 (1H, d, J= 12 HZ), 8.92 (1H, s), 9.78 (1H, s).

^{13}C- NMR (100 MHz, d_6-DMSO):

δ 28.8, 56.1, 58.7, 66.9, 101.2, 103.5, 110.5, 111.7, 116.7, 120.8, 123.5, 128.3, 128.8, 129.1, 130.4, 130.8, 131.6, , 132.6, 136.7, 139.6, 141.3, 146.3, 146.6, 147.1, 148.7, 149.7, 151.8.

MALDI-MS: Calc. for $C_{26}H_{20}Cl_2NO_4^+$480.08; found 480.22

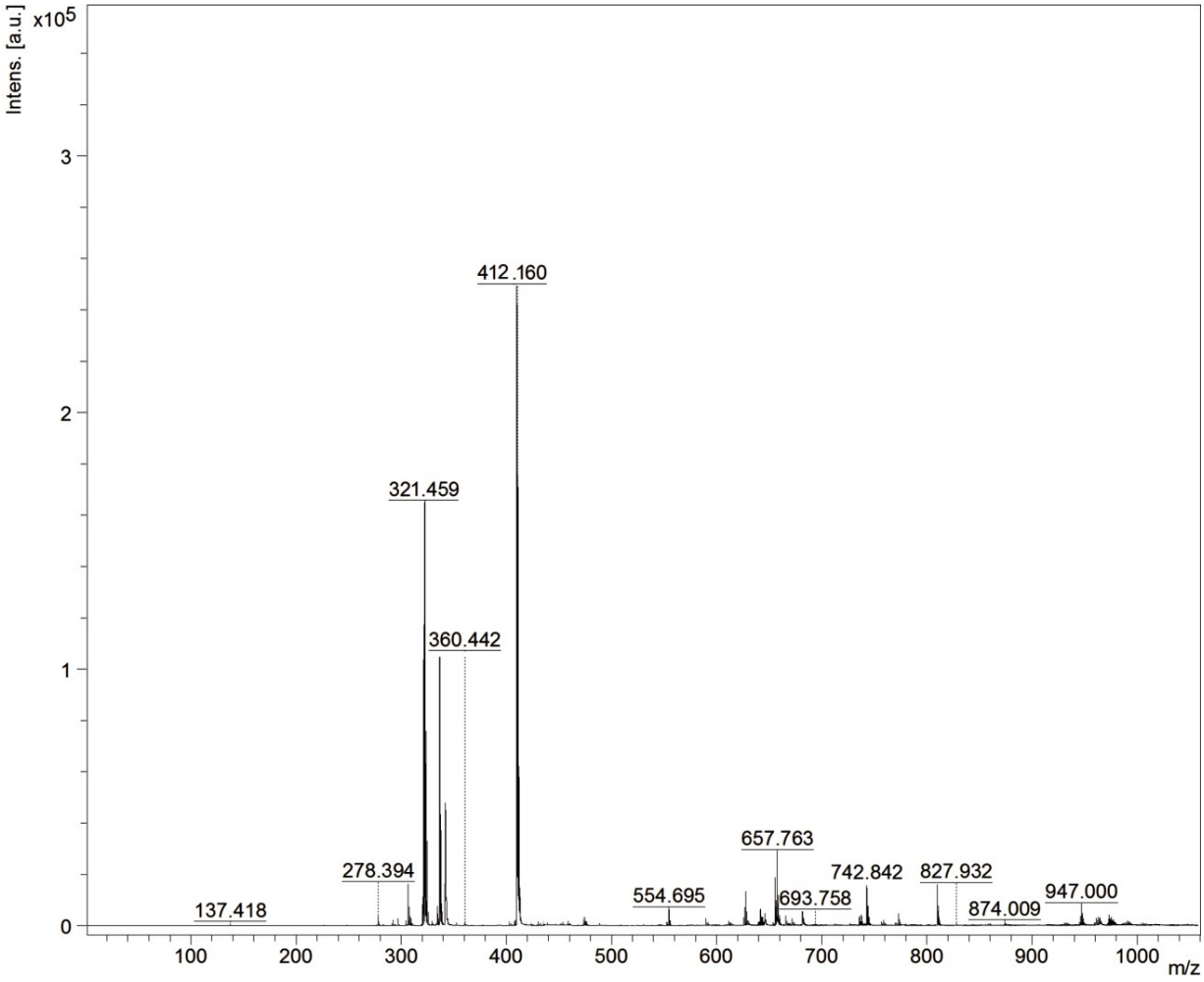

Fig. S27 MALDI-MS spectra of BZ_1

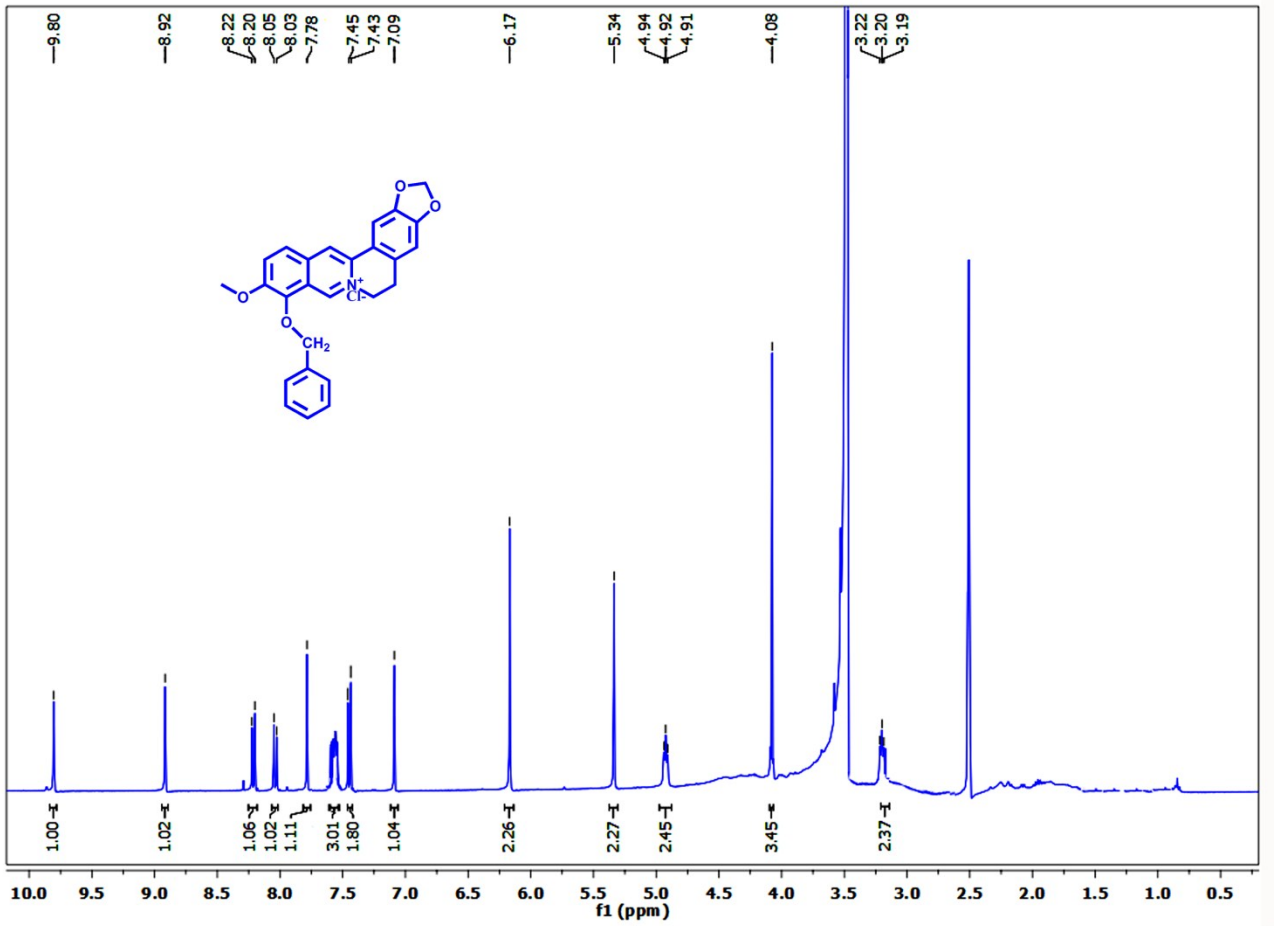

Fig. S28 ^{1}H NMR spectra of BZ_1 in d_6-DMSO.

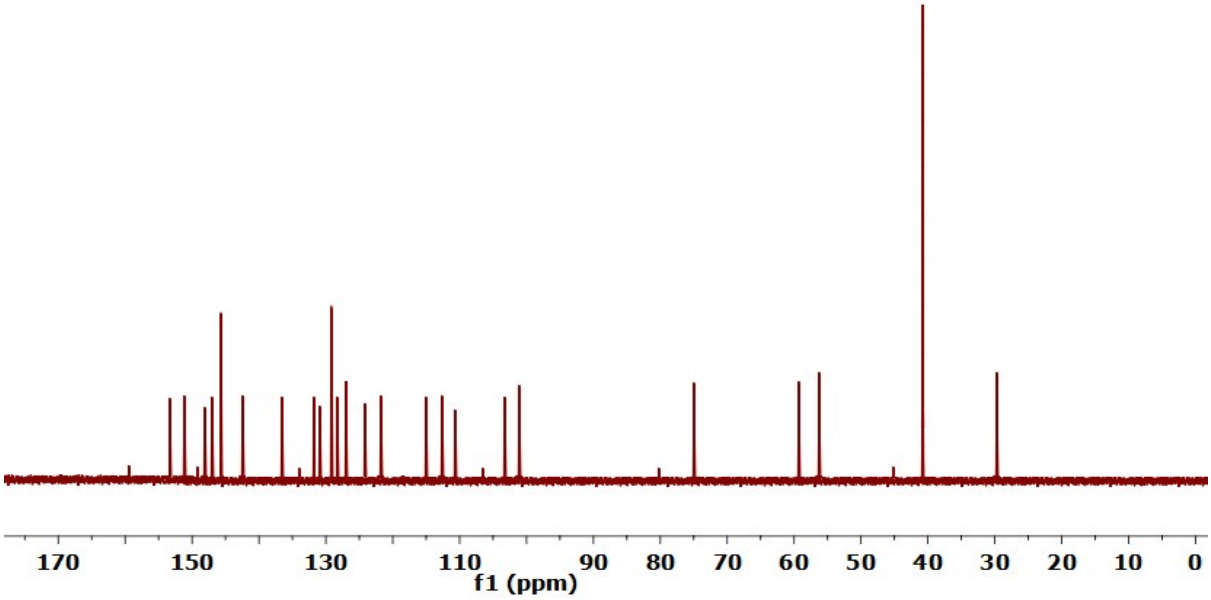

Fig. S29 ^{13}C NMR spectra of BZ_1 in d6-DMSO.

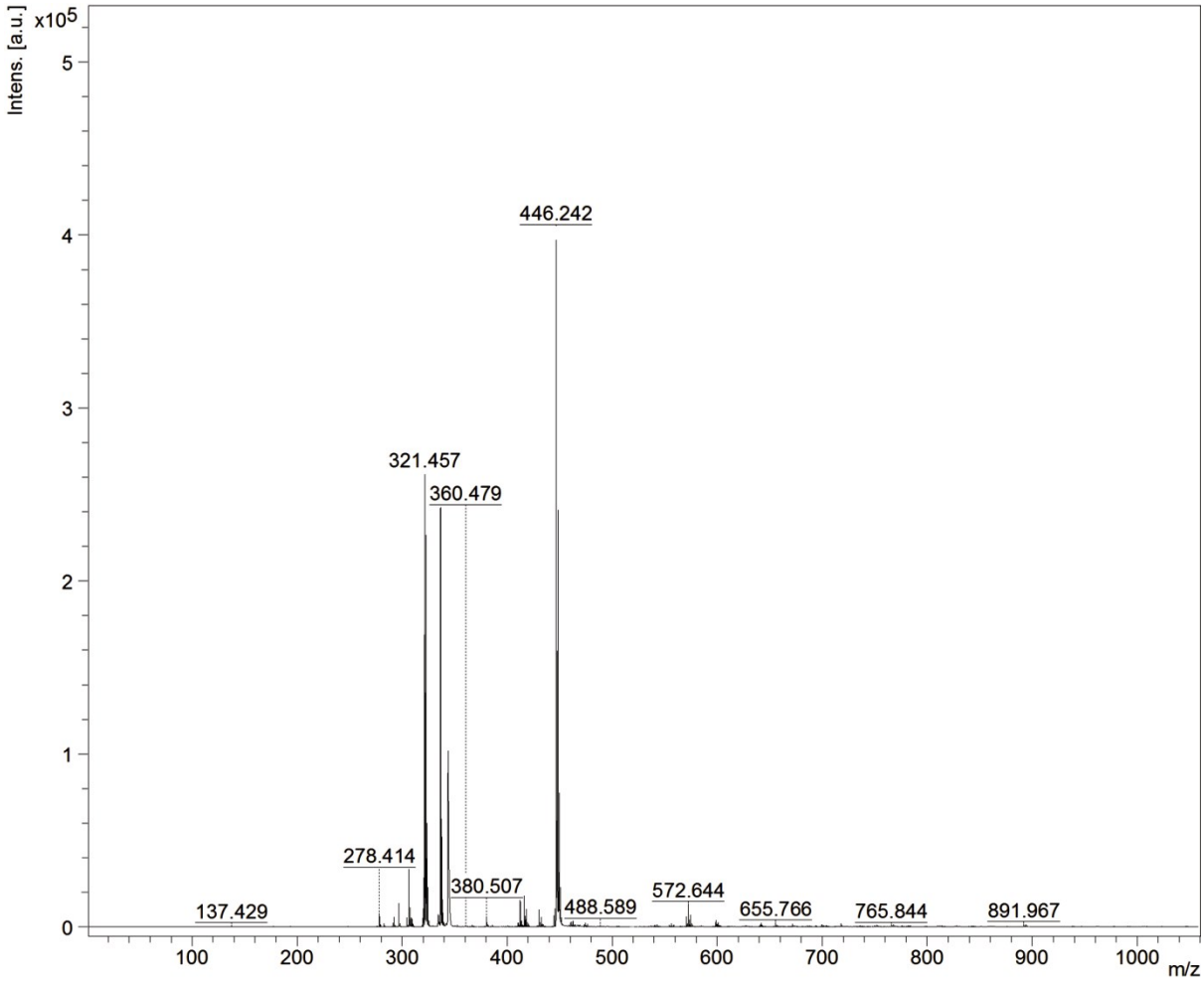

Fig. S30 MALDI-MS spectra of BZ_2

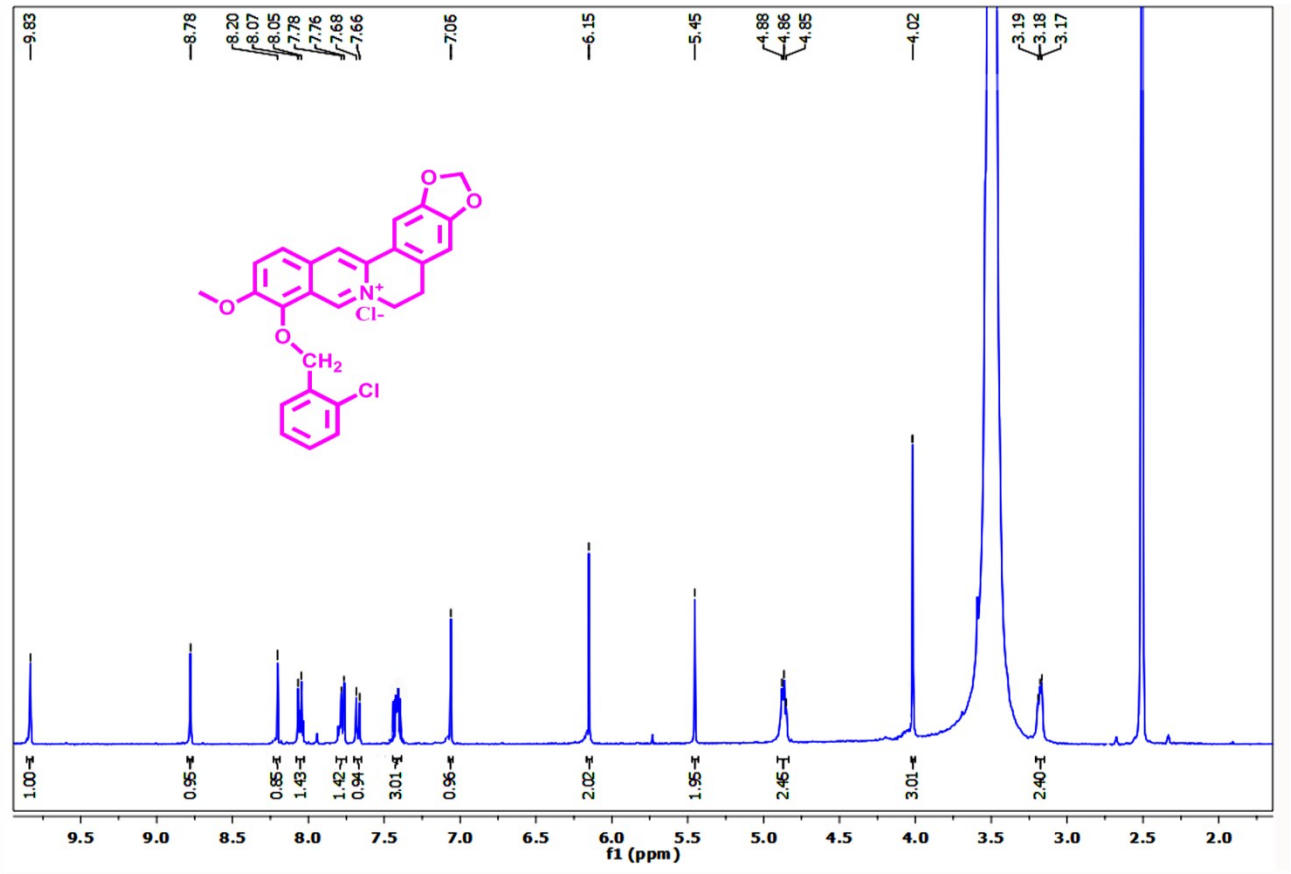

Fig. S31 ^{1}H NMR spectra of BZ_2 in d_6-DMSO

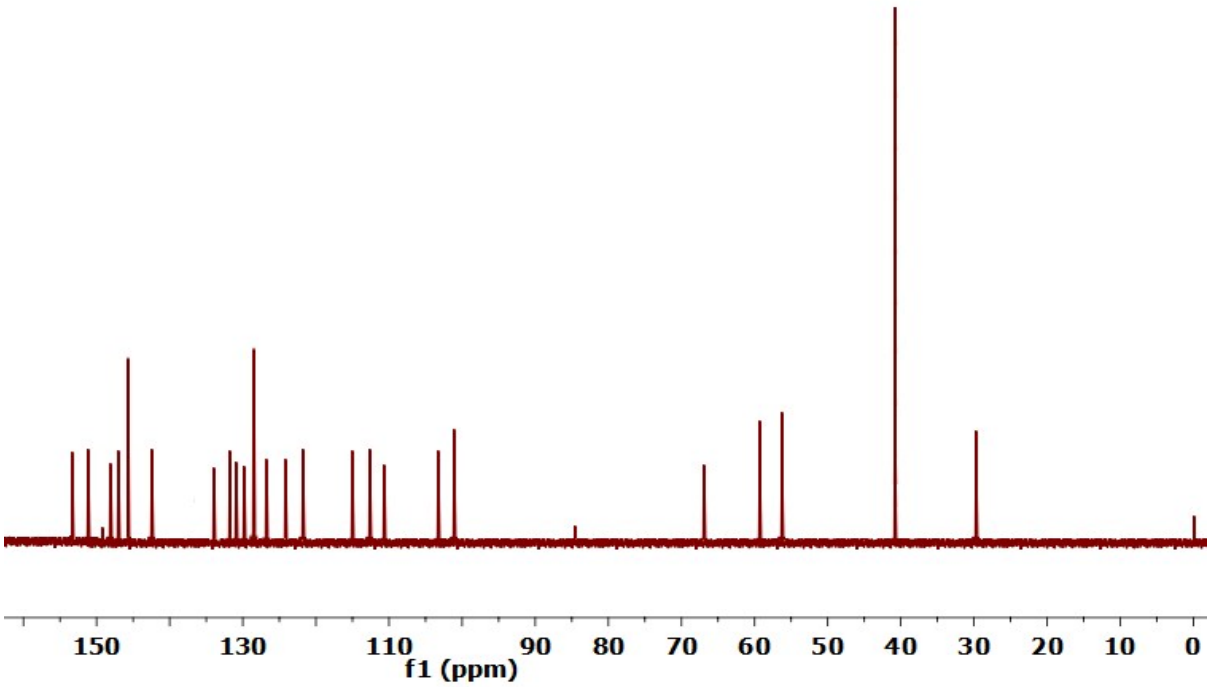

Fig. S32 ^{13}C NMR spectra of BZ_2 in d6-DMSO

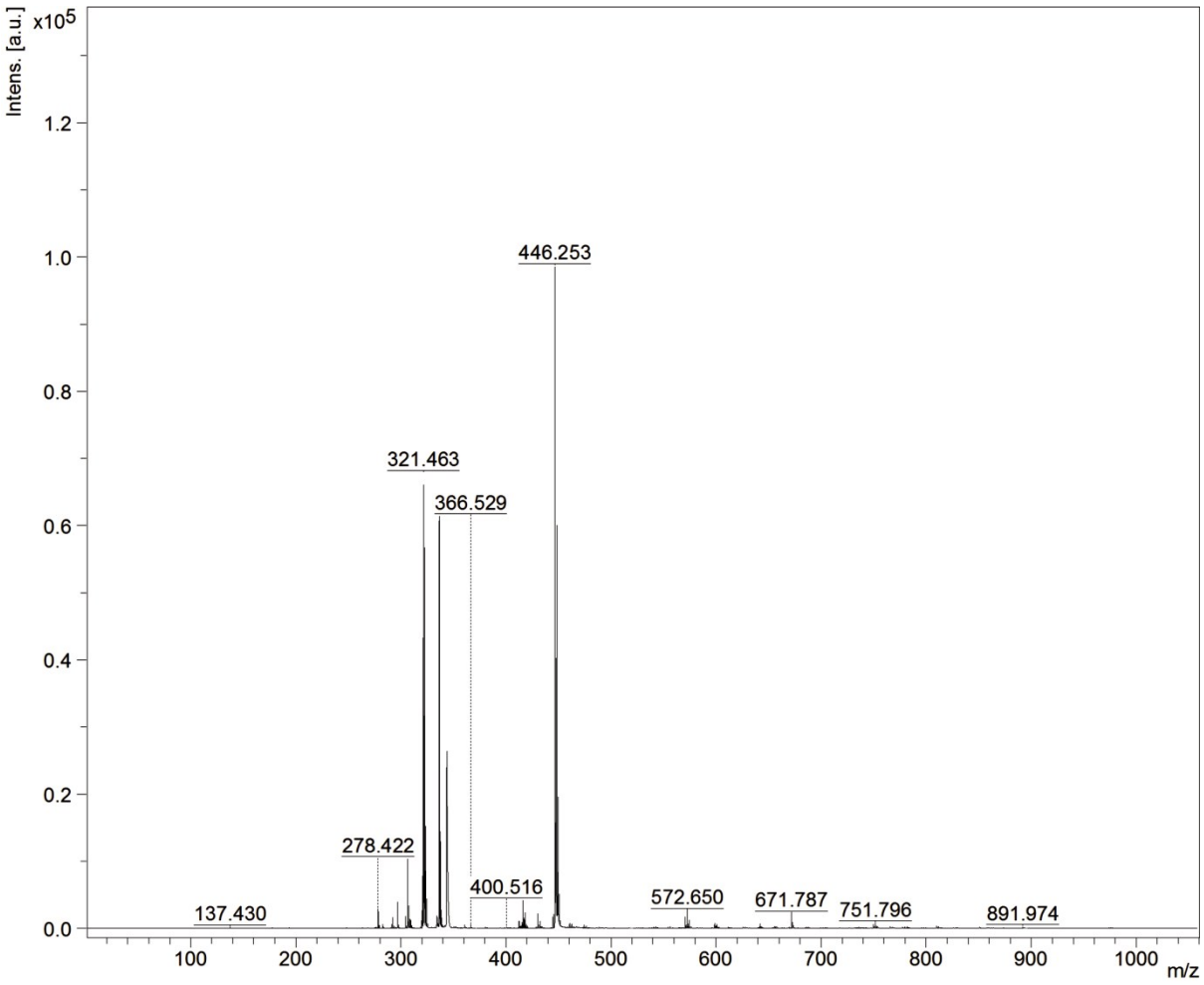

Fig. S33 MALDI-MS spectra of BZ_3

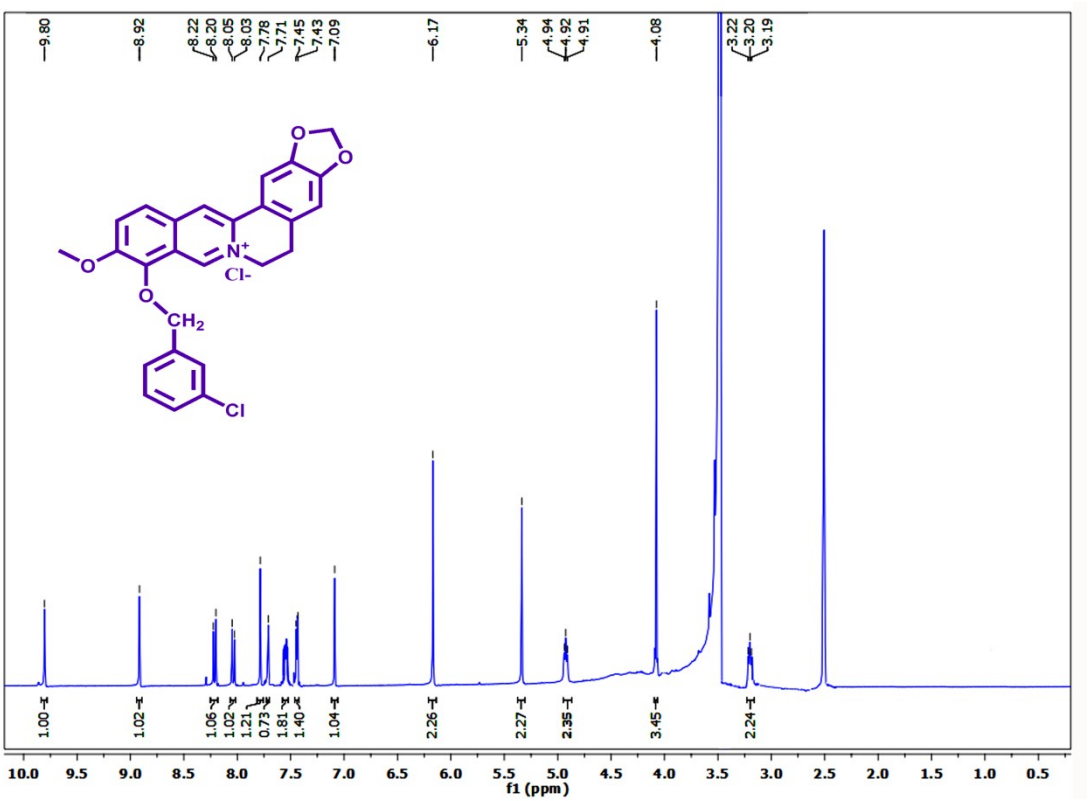

Fig. S34 ^{1}H NMR spectra of BZ_3 in d_6-DMSO

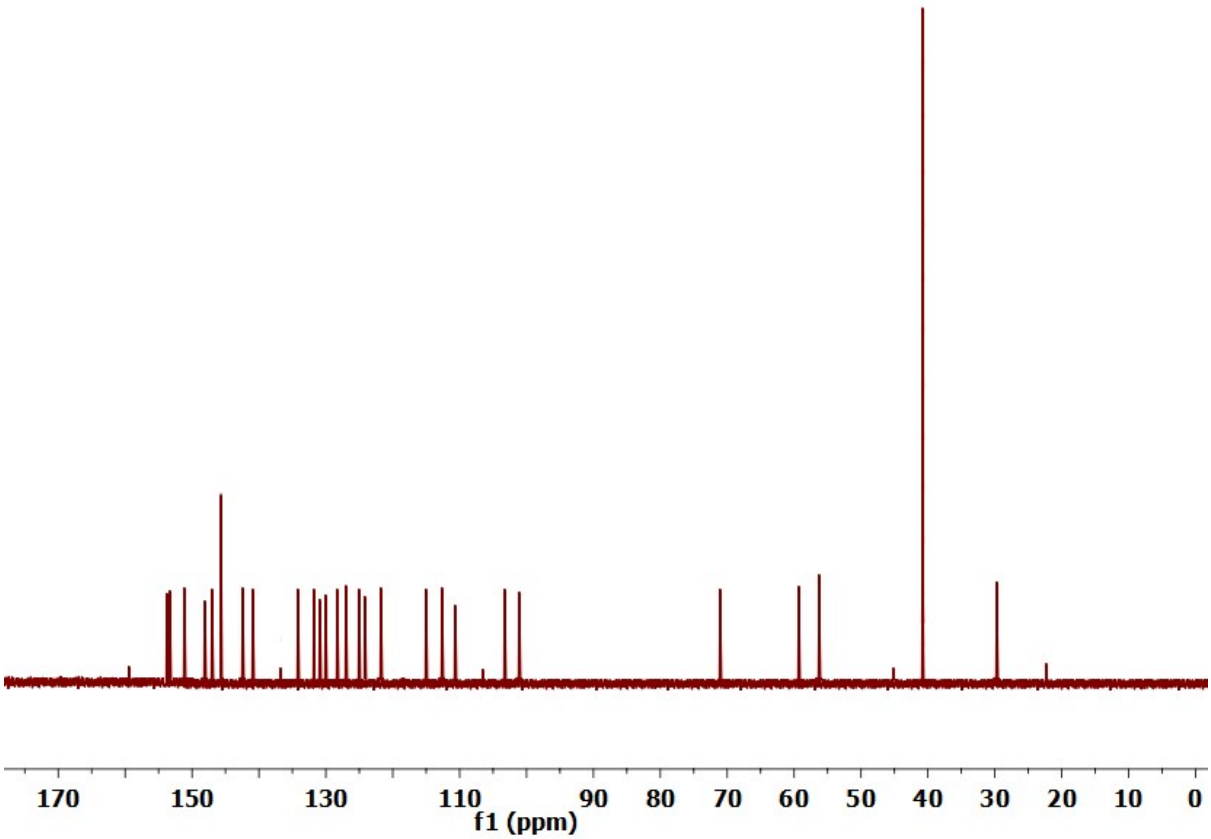

Fig. S35 ^{13}C NMR spectra of BZ_3 in d_6-DMSO

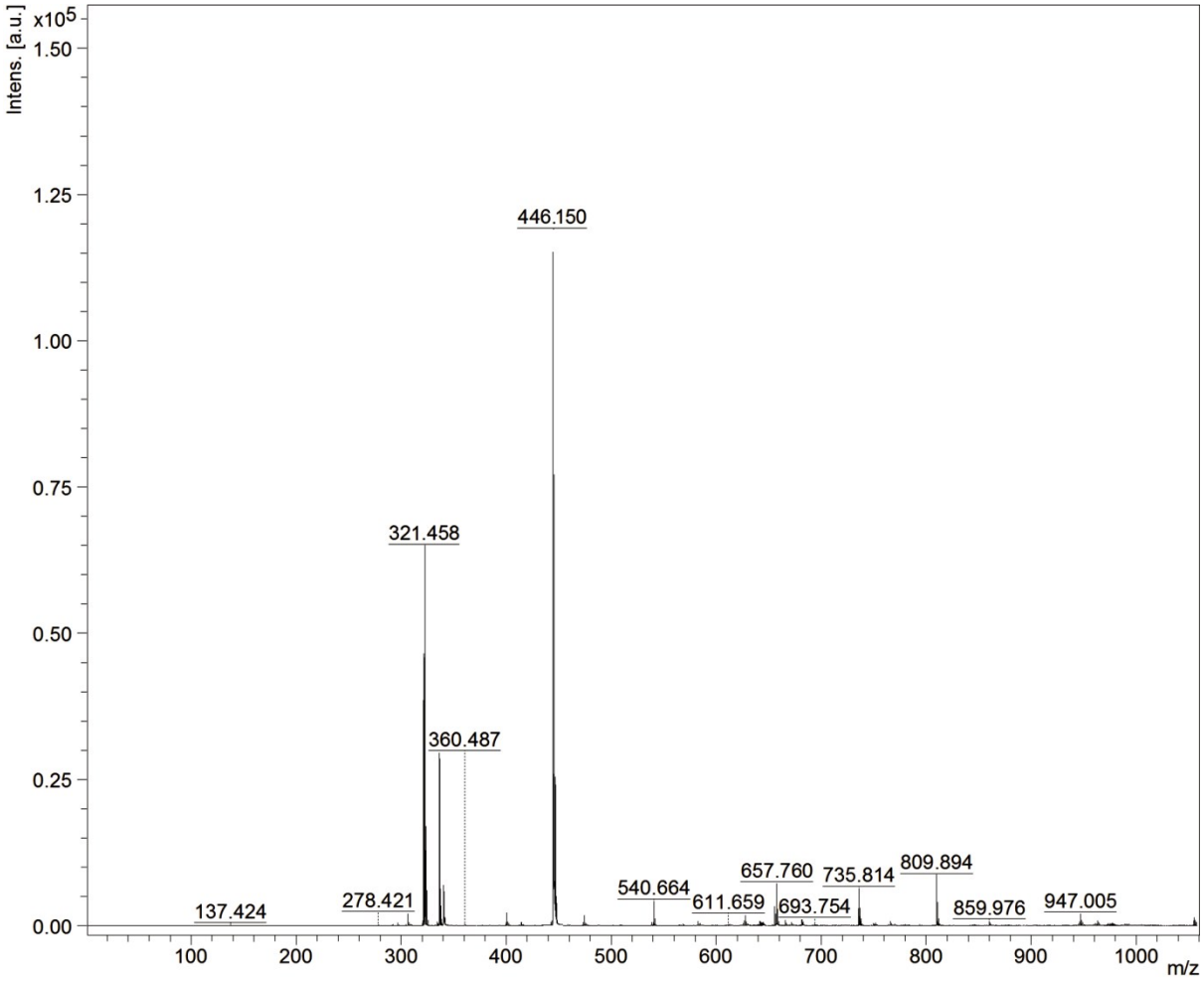

Fig. S36 MALDI-MS spectra of BZ_4

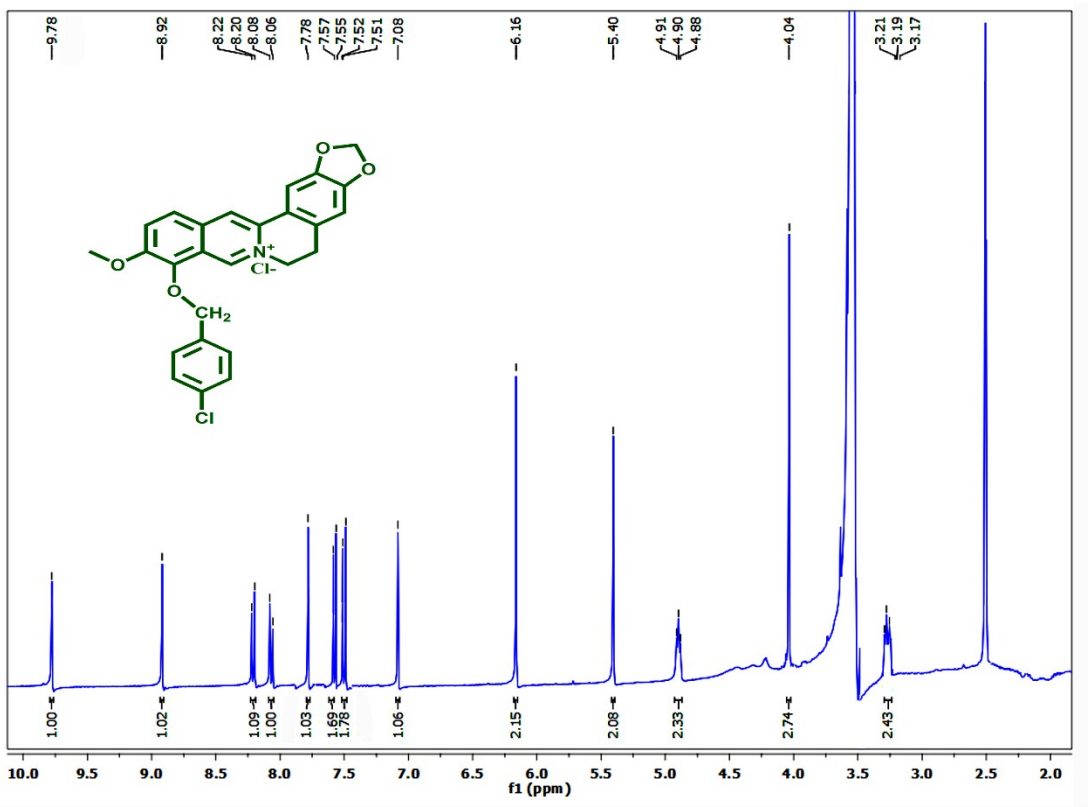

Fig. S37 ^{1}H NMR spectra of BZ_4 in d_6-DMSO

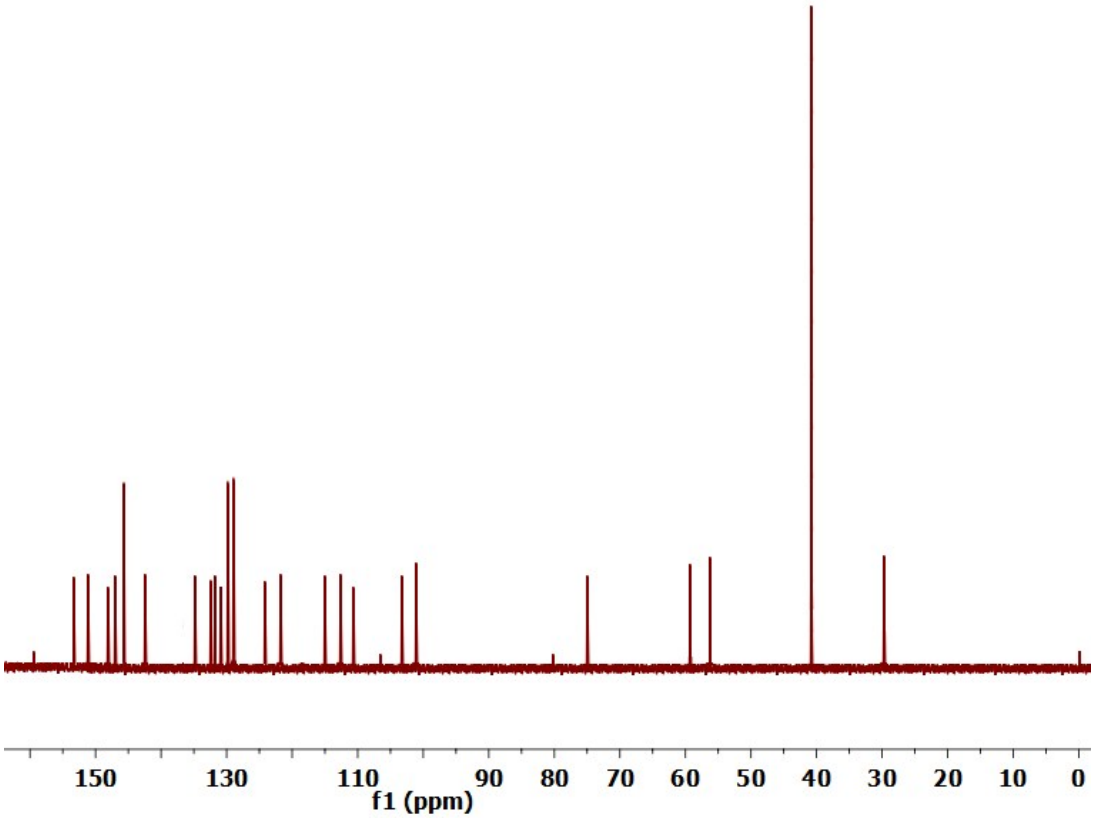

Fig. S38 ^{13}C NMR spectra of BZ_4 in d_6-DMSO.

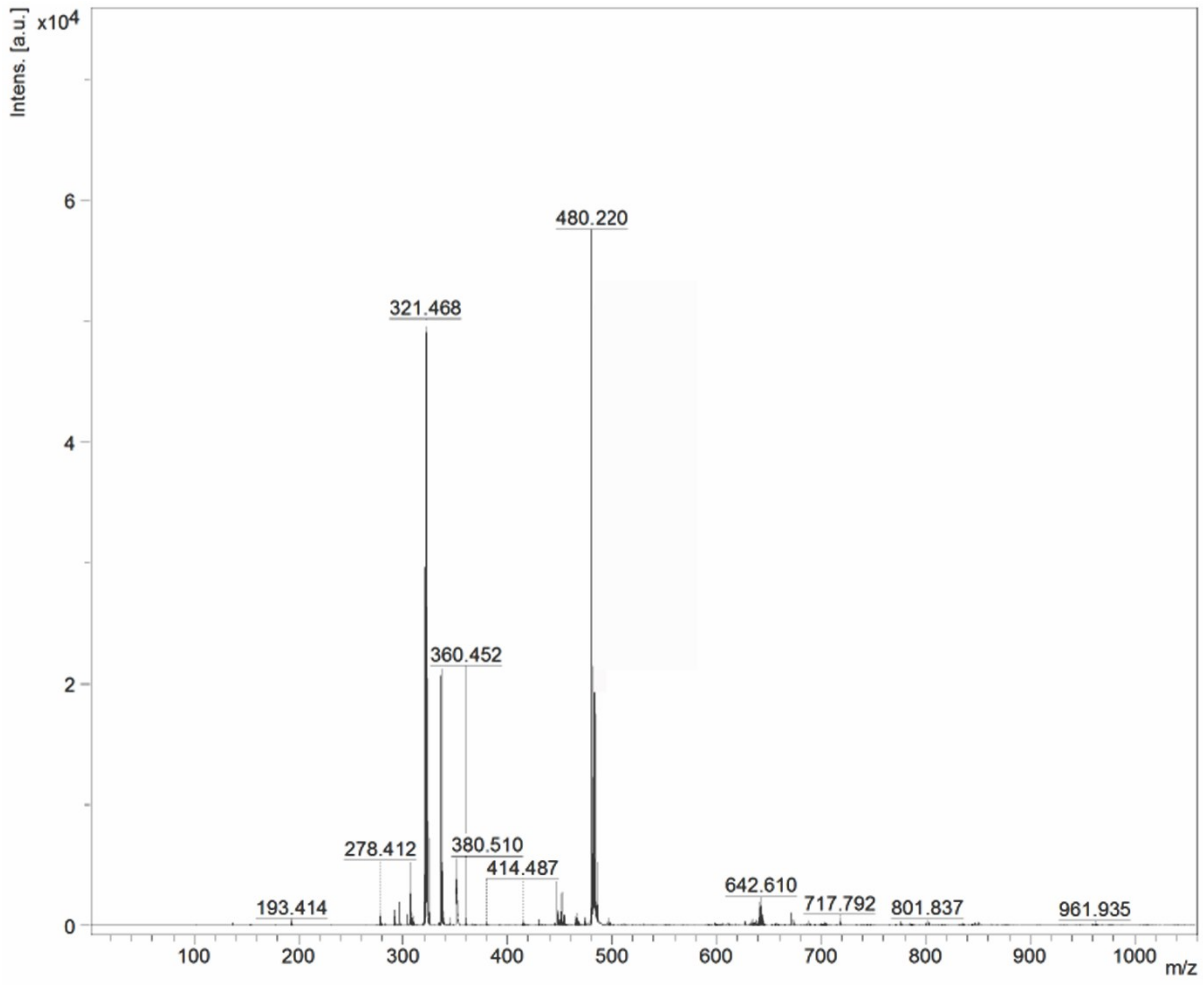

Fig. S39 MALDI-MS spectra of BZ_5

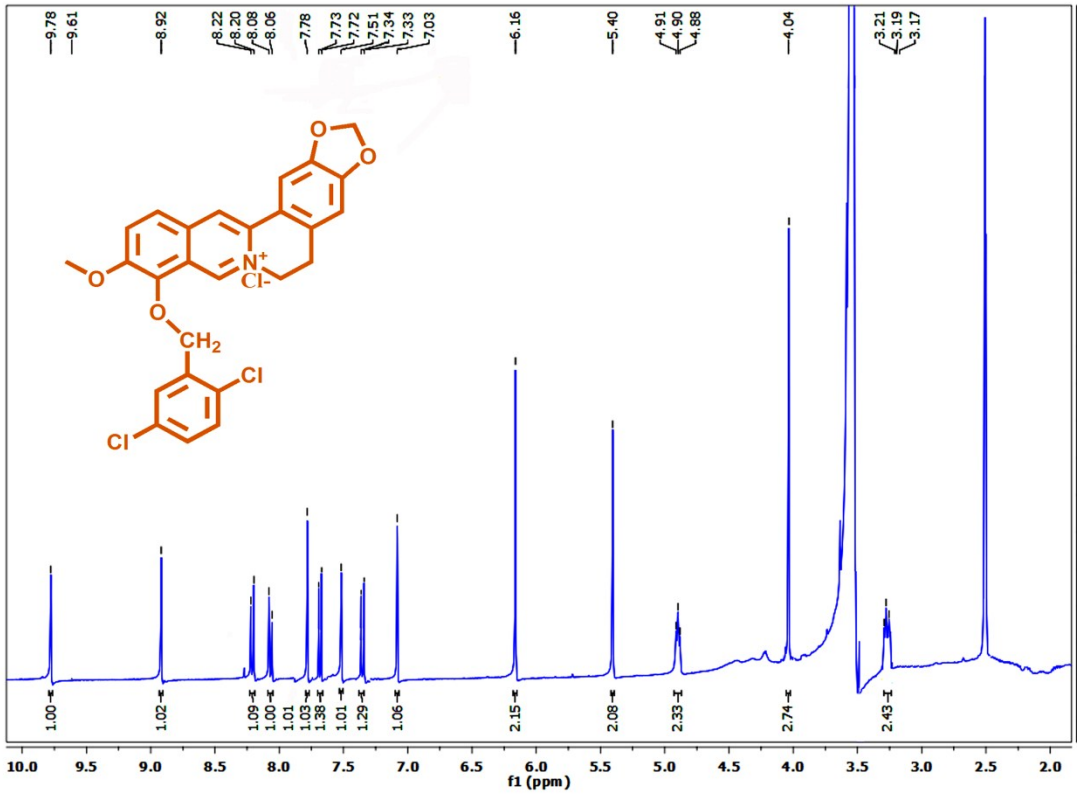

Fig. S40 ^{1}H NMR spectra of BZ_5 in d_6-DMSO

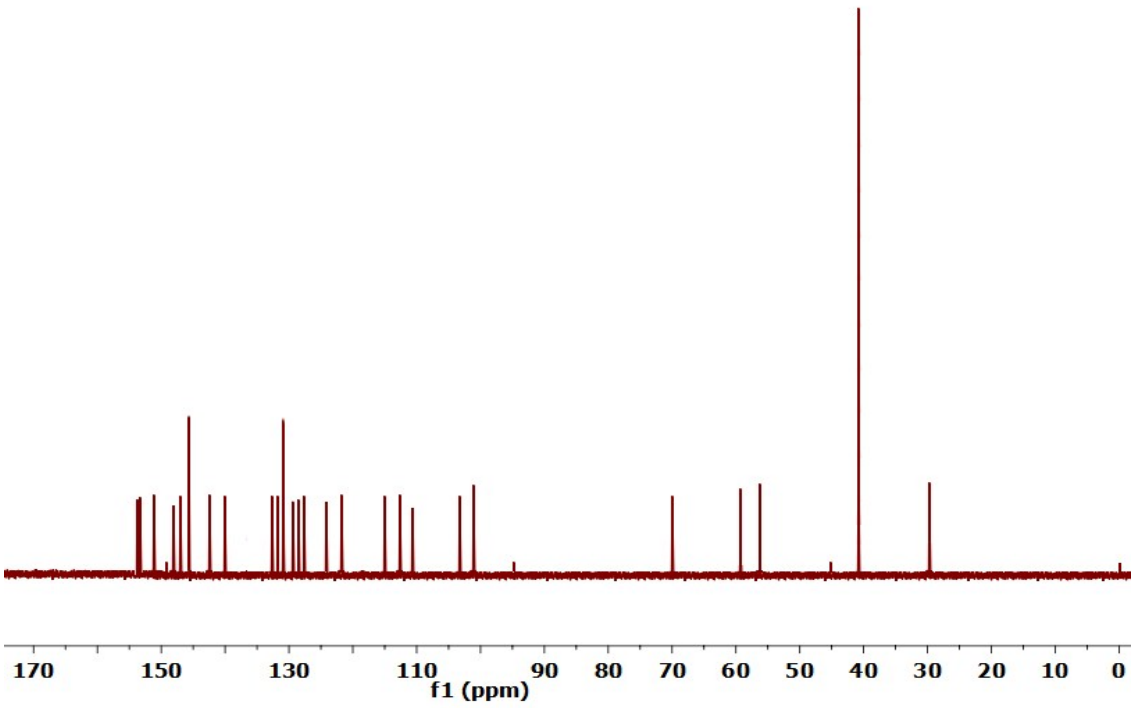

Fig. S41 ^{13}C NMR spectra of BZ_5 in d_6-DMSO.